Zbtb38 inhibits apoptosis by transcriptionally regulating *XIAP* expression

Eishou Matsuda[1]*, Toshiaki Shigeoka[1], Hiroyuki Nagaoka[2], Nunuk Aries Nurulita[3], Shogo Tada[1], Yasumasa Ishida[1], Yasumasa Bessho[4]

[1]Functional Genomics and Medicine, Nara Institute of Science and Technology, Ikoma, 630-0192, Japan

[2]Parexel International Inc. Tradepia Yodoyabashi, 2-5-8, Imabashi, Chuo-ku, Osaka-shi, Osaka 541-0042, Japan

[3]Faculty of Pharmacy, University of Muhammadiyah Purwokerto, Jalan Raya Dukuhwaluh PO BOX 202, 53052, Purwokerto, Central Java, Indonesia.

[4]Gene Regulation Research, Nara Institute of Science and Technology, Ikoma, 630-0192, Japan

*Correspondence: Eishou Matsuda (ematsuda@bs.naist.jp)

Telephone: +81-743-72-5559; FAX: +81-743-72-5559

Keywords

Apoptosis, XIAP, Bcl-2, ES cell differentiation, embryonic development, cancer.

Abstract

X-linked inhibitor of apoptosis protein (XIAP) is a key suppressor of apoptosis, a major form of programmed cell death critical for cellular differentiation, embryogenesis, and cancer development. Despite its importance, the upstream regulators and regulatory elements of *XIAP* are not well understood. This study provides evidence that the zinc finger transcription factor Zbtb38, a negative regulator of apoptosis, regulates *XIAP* expression in Zbtb38 loss- and gain-of-function experiments. Notably, XIAP overexpression rescued the apoptosis induced by *Zbtb38* knockdown, indicating that Zbtb38-mediated apoptosis is at least partially dependent on XIAP. Chromatin immunoprecipitation and luciferase assays revealed that Zbtb38 binds to and activates E-boxes within the *XIAP* enhancer, underscoring the critical role of these E-boxes in *XIAP* expression. Additionally, Zbtb38 loss during embryonic stem (ES) cell differentiation and embryogenesis resulted in increased apoptosis and decreased expression of XIAP and Bcl-2, highlighting their importance in these processes. Furthermore, Zbtb38 downregulation induced apoptosis in cancer cells lacking p53 expression, suggesting that Zbtb38 could be a potential therapeutic target in cancer.

Introduction

In mammals, apoptosis is a genetically regulated form of programmed cell death critical for maintaining homeostasis by eliminating damaged or unnecessary cells[1][2]. It also plays an important role in the immune system by removing infected and cancerous cells[3]. Intrinsic apoptosis, referred to here as apoptosis, is triggered by internal signals such as DNA damage, hypoxia, hydrogen peroxide, and lack of survival factors[4][5]. Once these signals are detected, initiator caspase-9 is activated to its active form, cleaved caspase9 (cCasp9), leading to the activation of downstream effector caspases, such as caspase-3 and caspase-7 (cCasp3 and cCasp7)[6][7]. This cascade results in the cleavage of several hundred cellular substrates, of which PARP is the best known, ultimately leading to irreversible apoptosis[8].

The Bcl-2 family of proteins regulates the release of apoptogenic proteins from mitochondria. This family includes anti-apoptotic proteins (Bcl-2, Mcl-1, Bcl-xL, and Bcl-w), BH3-only pro-apoptotic proteins (Bik, Bid, Bad, Bim, Noxa, and Puma), and multidomain pro-apoptotic proteins (Bax and Bak) [9]. BH3-only pro-apoptotic proteins bind to and inhibit anti-apoptotic proteins[10][11]. Bcl-2, one of the most studied anti-apoptotic genes, inhibits apoptosis by binding to and sequestering pro-apoptotic proteins such as Bax and Bak, preventing the release of cytochrome c from mitochondria[12] [13]. Another critical regulator of apoptosis is p53, which activates pro-apoptotic proteins (Noxa and Puma), inhibits anti-apoptotic proteins (Bcl-2 and Bcl-xL), and interacts directly with the mitochondrial membrane [14]. The multifaceted functions of p53 in apoptosis highlight its importance as a tumor suppressor and relevance to cancer biology[15].

In contrast to the Bcl-2 family, members of the inhibitor of apoptosis (IAP) gene family act as endogenous inhibitors of caspases. The IAP family is divided into three classes: Class 1 (cIAP1, cIAP2, and XIAP), Class 2 (NAIP), and Class 3 (survivin and Bruce) [16][17]. Class 1 IAPs contain three baculovirus IAP repeat (BIR) domains that allow the direct binding and inhibition of caspases. XIAP uniquely inhibits caspases at physiological concentrations, distinguishing it from cIAP1 and cIAP2[18][19]. Single knockout (KO) mice (*XIAP*, *cIAP1*, and *cIAP2*) and double knockout mice (*XIAP*/*cIAP2*) were viable and fertile[20][21], whereas double knockout mice (*XIAP/cIAP1* or *cIAP1/cIAP2*) died at approximately embryonic day 10.5 (E10.5), indicating the redundancy of these proteins [21][22]. In contrast, IAP inhibitors such as Smac and Xaf1 bind to the BIR domains of IAPs, displacing caspases from these inhibitory proteins[23]. Htra2, another IAP inhibitor, degrades IAPs via serine protease activity, neutralizing their inhibitory effects on caspases[24]. Despite the critical role of XIAP in inhibiting apoptosis, its upstream regulators and regulatory elements remain largely unknown.

Previously, we and others have demonstrated that Zbtb38, also known as CIBZ, binds to methylated CpG or non-methylated DNA through the first zinc finger cluster (ZF1-5) to either repress or activate transcription[25][26][27][28][29]. Our previous study showed that Zbtb38 promotes the proliferation of mouse ES cells and inhibits their differentiation toward the mesodermal lineage[30][31]. We have shown that siRNA-mediated knockdown (KD) of *Zbtb38* induces apoptosis

in murine cells, as evidenced by the upregulation of cCasp9, cCasp3, cCasp7 and cleaved PARP (cPARP), as well as the increased uptake of annexin V[32]. We also found that the loss of *Zbtb38* (KO and KD) in ES cells resulted in decreased proliferation without inducing apoptosis, demonstrating that Zbtb38-associated apoptosis is cell type-dependent[30]. Cai et al. reported that overexpression of Zbtb38 reduced apoptosis and restored spinal cord function in mice after spinal cord injury[33]. Recently, we reported that loss of one allele of *Zbtb38* in the germline results in increased apoptosis shortly after implantation, leading to early embryonic lethality at E9.5[34]. Despite the critical role of Zbtb38 in apoptosis, the underlying mechanisms remain unclear.

The aim of this study was to identify the targets of Zbtb38 during apoptosis and to elucidate the underlying molecular mechanisms. To this end, we performed comparative analyses of gene expression changes in Zbtb38 loss- and gain-of-function experiments in p53-expressing and p53-deficient cells, including ES and cancer cells. *Zbtb38* KD/KO and its overexpression in various cell lines coincided with changes in *XIAP* expression, suggesting that *XIAP* is a potential target of Zbtb38. By analyzing the upstream region of the *XIAP* promoter, we identified two E-box motifs (CANNTG) located 4-5 kb from the transcription start site (*TSS*). Molecular biology techniques revealed that Zbtb38 binds to these E-boxes and activates *XIAP* transcription. Finally, decreased expression of *XIAP* and *Bcl-2,* induced by Zbtb38 loss, was observed in ES cells and during embryogenesis, suggesting that these factors are essential for these biological processes.

STATEMENT

All experiments were approved by the Nara Institute of Science and Technology and were conducted according to the guidelines of the Science Council of Japan.

Materials and methods

Generation of *Zbtb38* heterozygous (Δ*fl*/+) mice

Zbtb38 Δ*fl*/+ mice were generated by crossing *Zbtb38 fl/fl* mice with CAG-Cre mice, and genotyping was performed as described previously[34]. The CAG-Cre mice were provided by Dr. Masaru Okabe (Osaka University, Osaka, Japan). Wild-type (C57BL/6J) mice were purchased from CLEA (Tokyo, Japan). All animal experiments were approved by the Animal Care Committee of the Nara Institute of Science and Technology and conducted in accordance with the guidelines of the Science Council of Japan.

Cell Culture and ES cell differentiation assay

C2C12 cells were cultured in Dulbecco's modified Eagle's medium (DMEM; Nacalai Tesque) supplemented with 15% fetal bovine serum (FBS; Sigma-Aldrich), 2 mM L-glutamine (Nacalai Tesque), and 1% penicillin/streptomycin (Nacalai Tesque) as previously described[28]. *p53* KO and *p53/Dnmt1* double knockout (DKO) MEFs were kindly provided by Dr. Richard Meehan (Medical Research Council Human Genetics Unit, Edinburgh, UK). Immortalized MEFs, hereafter referred to as MEFs, were generated in our laboratory by stably transfecting MEF derived from C57BL/6 mice with SV40 large T antigen. MEFs, *p53* KO MEFs, and *p53/Dnmt1* DKO MEFs were cultured in the above medium, supplemented with 10% FBS and 1 mM sodium pyruvate (Invitrogen). NMuMG, 4T1, and 293T cells were cultured in DMEM supplemented with 10% FBS, 2 mM L-glutamine and 1% penicillin/streptomycin as previously described[25].

The generation and culture of mouse RF8 (wild-type) ES and *Zbtb38* KO ES cells have been described previously[30]. Briefly, undifferentiated ES cells were grown on mitomycin C-treated SNL-STO cells with medium (DMEM, 15% FBS, 2-mM L-glutamine, 100 μM non-essential amino acids, 1% penicillin and streptomycin, and 0.1-μM β-mercaptoethanol with 1000 IU/ml leukemia inhibitory factor (LIF) and the differentiation inhibitors 3i (3 μM CHIR99021, 1 μM PD0325901, and 10 μM SB431542; Selleck Chemicals). To induce differentiation, ES cells were cultured in ES medium without LIF and 3i to form embryoid bodies (EBs) in suspension, as described in our previous methods[31].

Reporter constructs and luciferase assays

To generate the pGL3-XIAP 4.7 kb construct, genomic DNA from C2C12 cells was amplified by PCR using primers (listed in the Supplementary Table) containing *Kpn*I and *Xho*I restriction sites. The 4.7 kb fragment was ligated into predigested pGL3 vectors using the same restriction enzymes. Site-directed mutagenesis (Takara) was used to generate E-box mutants (pGL3-XIAP m1 and pGL3-XIAP m1/m2) according to the manufacturer's instructions. The primers used to construct these mutants are listed in the Supplementary Table. DNA sequences were verified using an

automated sequencer (ABI PRISM 3130). Plasmid (pcDNA3-Flag, pcDNA3-Flag-Zbtb38, pcDNA3-Myc, pcDNA3-Myc-Zbtb38, and pcDNA3-Myc-Zbtb38 ΔZF1-5) were constructed as previously described[25].

Luciferase assays were performed as described previously[31]. Briefly, HEK293T cells were transfected with 0–250 ng of expression plasmids for Flag or Flag-fusion proteins and 100 ng of firefly luciferase reporters (pGL3 vector, pGL3-XIAP constructs) in a 24-well plate. Four nanograms of the pRL-TK reporter was used as an internal control, and the total amount of expression plasmids was standardized to that of the pcDNA3. Firefly luciferase activity was normalized to the transfection efficiency based on the luciferase activity of the internal control. Cells were subjected to luciferase assay using the Dual-Luciferase Reporter Assay System (Promega) 32–48 h after transfection. Assays were performed in duplicate in three independent experiments.

siRNA and transient transfection

Cells were transfected with 5–10 nM *Zbtb38*-specific Dicer substrate siRNA duplex or scrambled negative control (Integrated DNA Technologies) as previously described[32]. Transfection was performed using INTERFERin reagent (Polyplus Transfection) or RNAiMAX (Thermo Fisher Scientific) according to the manufacturer's instructions. siRNA-transfected cells were used for semiquantitative RT-PCR, qRT-PCR, and immunoblotting 24–48 h after transfection. Transient transfections were performed using Lipofectamine 2000 (Invitrogen), PEI-Max (Polysciences), or Viafect (Promega), according to the manufacturer's instructions. Briefly, cells were transfected with pcDNA3-Flag and pcDNA3-Flag-tagged Zbtb38 series, pcDNA3-Myc and pcDNA3-Myc-Zbtb38 series for 24–48 h before harvesting.

RNA extraction, qRT-PCR and semiquantitative RT-PCR

Total RNA was extracted from various cell lines using Sepasol RNA Super G (Nacalai Tesque) for cultured cells and PicoPure RNA Isolation Kit (Thermo Fisher Scientific) for E7.5 embryos, according to the manufacturer’s instructions. Approximately 5 ng of total RNA from E7.5 embryos, and 500 ng of total RNA from cultured cells were used to synthesize cDNA using ReverTra Ace qPCR RT Master Mix with gDNA Remover (TOYOBO). qRT-PCR was performed using a LightCycler® 96 System (Roche Diagnostics) with Thunderbird SYBR Green PCR Mix (TOYOBO), as previously described[31]. *GAPDH* was used as the reference gene, and all analyses were performed using the 2-deltadelta Ct method with Roche LightCycler 96 system software. Semi-quantitative RT-PCR was performed at an annealing temperature of 58 °C as described previously[31]. Reaction products were separated on a 2% agarose gel and visualized by ethidium bromide staining. *GAPDH* was used as an internal control for both qRT-PCR and semiquantitative RT-PCR, and the primer sequences are listed in the Supplementary Table.

Western Blotting

Western blotting was performed as previously described [25]. Briefly, protein lysates were prepared in a radioimmunoprecipitation assay (RIPA) buffer supplemented with a complete protease inhibitor (Roche). Proteins were separated by 6–15% SDS-PAGE, transferred to PVDF membranes,

and probed with antibodies against Zbtb38[25], XIAP (M044-3, MBL), Bcl-2 (D038-3, MBL), and GAPDH (60004-1-Ig, Proteintech). Antibodies against cleaved caspase-3 (cCasp3, #9664) and cleaved PARP (cPARP, #9542) were purchased from Cell Signaling Technology. The expected molecular sizes are Zbtb38 (175 kDa), XIAP (55 kDa), Bcl-2 (26 kDa), cPARP (89 kDa), cCasp3 (17 kDa), GAPDH (36 kDa), and GAPDH was used as an internal control. Horseradish peroxidase (HRP)-conjugated anti-mouse (#7076) or anti-rabbit IgG (#7074) secondary antibodies were purchased from Cell Signaling Technology. Detection and quantification were performed using a chemiluminescence imaging system (FUSION, Thermo Fisher Scientific).

ChIP assay and ChIP-qPCR

ChIP assays were performed as described previously[28][31]. Briefly, subconfluent C2C12 cells or *p53* KO MEFs were cross-linked with 1% formaldehyde and 0.125 M glycine for 15–30 min, washed three times with ice-cold phosphate-buffered saline (PBS), and harvested with SDS lysis buffer. Chromatin lysate was sonicated on ice to obtain an average DNA length of 500 bp. After pre-clearing the lysates with Protein G Sepharose beads, an anti-Zbtb38 antibody was used to immunoprecipitate the protein-DNA complexes, and preimmune IgG was used as a negative control. Input DNA (2%), IgG-precipitated DNA, and Zbtb38-immunoprecipitated DNA were amplified by qRT-PCR. qRT-PCR data are presented relative to the input control, and primers are listed in the Supplementary Table. Each experiment was performed three times.

TUNEL assay

Terminal deoxynucleotidyl transferase (TdT)-mediated dUTP nick-end labeling (TUNEL) assay (#8445, MBL) was performed as previously described[34]. Briefly, paraffin-embedded tissue sections were deparaffinized, DNA nick-end labeled, counterstained with 1 μg/ml Propidium Iodide (PI), and mounted. Slides were analyzed using a TCS SP8 confocal microscope (Leica).

Quantification and Statistical analysis

Statistical analyses were performed with GraphPad Prism 10 and Microsoft Excel. Unless otherwise indicated, data from at least three independent experiments, each performed in triplicate, are presented as mean ± SEM. An unpaired two-tailed Student's *t*-test was used to compare two groups, and ANOVA was used to compare more than two groups. Statistical significance was determined at $*p < 0.05$, $**p < 0.01$, and $***p < 0.001$; "ns" indicates no significance ($p > 0.05$).

Results

Loss of Zbtb38-induced apoptosis is independent of p53 expression and DNA methylation, and *XIAP* is a target of Zbtb38

Our previous results showed that two siRNA-mediated *Zbtb38* knockdowns induced apoptosis in C2C12 cells and in *p53* KO mouse embryonic fibroblasts (MEFs), but the specific target remains unclear. To investigate further, we examined MEFs, *p53* KO MEFs, *p53/Dnmt1* DKO MEFs, myoblast C2C12 cells and mouse mammary cell lines (NMuMG and stage IV malignant 4T1). These were categorized as p53-expressing (MEF, NMuMG, and C2C12) and p53-deficient (p53 KO, 4T1, and DKO). qRT-PCR data showed that Zbtb38 knockdown resulted in decreased *XIAP* expression in all cell lines, decreased *Bcl-2* expression in NMuMG and C2C12 cells, and reduced *cIAP1* and *Mcl-1* expression in C2C12 cells (Figure 1). In contrast, the expression levels of other IAP genes (*cIAP2*, and *survivin*) and IAP inhibitor genes (*Smac*, *Htra2*, and *Xaf1*) were either minimally affected or unchanged (Figure 1). In addition, *Zbtb38* knockdown upregulated apoptotic genes, such as *Bak* in 4T1 cells, *Bik* in MEFs and DKO MEFs, and *Noxa* in *p53* KO and DKO MEFs. In DKO MEFs, loss of *Zbtb38* increased the expression of *Bcl-xL*, *Bcl-w*, *Bax*, *Bak* and *Puma* (Figure 1). Taken together, the consistent reduction of *XIAP* expression upon *Zbtb38* knockdown suggests that *XIAP* is a potential target of Zbtb38.

Immunoblotting analysis showed that siRNA-mediated *Zbtb38* knockdown decreased XIAP expression and induced apoptosis, as evidenced by increased levels of cCasp3 and cPARP, in all of the above cell lines, regardless of p53 expression (Figure 2A–2D, Supplementary Figure 1A–1B). These results, together with the finding that *Zbtb38* knockdown did not increase *p53* expression (Figure 1), indicate that p53 expression is not essential for Zbtb38-associated apoptosis. In addition, semi-quantitative PCR analysis revealed that *Zbtb38* overexpression or knockdown in C2C12 cells was positively correlated with *XIAP* expression, whereas the expression of *survivin* and IAP inhibitor genes remained minimally altered (Supplementary Figure 2). Because Zbtb38 functions as a methyl-CpG-binding protein, we investigated its potential dependence on DNA methylation. The results showed that *Zbtb38* knockdown also induced apoptosis in DKO MEFs, where DNA methylation was almost abolished due to Dnmt1 deficiency, suggesting that DNA methylation is not critical for Zbtb38-associated apoptosis. Since *Zbtb38* knockdown induced apoptosis in cancerous 4T1 cells (Figure 2D), suggesting that its knockdown has potential therapeutic effects in cancer. Collectively, these results strongly suggest that *XIAP* is a direct target of Zbtb38 in the regulation of apoptosis.

Zbtb38-associated apoptosis depends, at least in part, on XIAP expression

Since loss of Zbtb38 induces apoptosis along with a decrease in XIAP expression, suggesting that Zbtb38 overexpression suppresses apoptosis and increases XIAP expression. To confirm this, we examined XIAP expression and apoptotic status in p53-expressing and p53-deficient cells overexpressing Zbtb38. In C2C12 cells, immunoblotting analysis showed that Flag-Zbtb38 overexpression resulted in increased XIAP expression and decreased serum deprivation-induced upregulation of cCasp3 and cPARP, compared to cells expressing the Flag tag alone (Figure 3A). In

p53 KO MEFs, Flag-Zbtb38 overexpression increased XIAP expression and decreased both serum deprivation and hydrogen peroxide (H2O2)-induced apoptosis (Figure 3B–3C). To investigate whether *Zbtb38* knockdown-induced apoptosis depends on decreased XIAP expression, a rescue experiment was performed. In C2C12 cells, the induction of cCasp3 and cPARP by *Zbtb38* knockdown was dose-dependently attenuated by XIAP overexpression (Figure 3D). In *p53* KO MEFs, overexpression of either XIAP or Flag-XIAP significantly inhibited apoptosis induced by *Zbtb38* knockdown (Figure 3E). These findings, together with the observation that XIAP overexpression did not increase Zbtb38 expression, suggest that *XIAP* is a downstream target of Zbtb38. Taken together, these results indicate that Zbtb38-mediated apoptosis is at least partially dependent on XIAP expression, regardless of p53 expression.

Zbtb38 binds to the E-box motifs in the *XIAP* enhancers and activates *XIAP* transcription

To explore whether Zbtb38 binds to the *XIAP* promoter, a chromatin immunoprecipitation (ChIP) assay was performed in C2C12 cells. Given the limited understanding of *XIAP* transcriptional regulation in mammals, we focused on four highly conserved regions (a, b, c, and d) within the upstream regulatory regions (RRs; Figure 4A). The results showed that Zbtb38 did not bind to the putative promoter regions (a and b) (Figure 4B). In contrast, Zbtb38 was enriched in the putative enhancer regions c and d, located approximately 4.5 kb and 4.7 kb upstream of the *TSS* of *XIAP*, respectively. This enrichment of Zbtb38 at enhancers (c and d) was also observed in *p53* KO MEFs (Supplementary Figure 3), indicating that Zbtb38 binds to *XIAP* enhancers, regardless of p53 expression.

To evaluate the transcriptional effect of Zbtb38 on the 4.7 kb RR of *XIAP*, a luciferase assay was performed using HEK293T and C2C12 cells, which express low and high levels of Zbtb38, respectively, as described [25][28]. Overexpression of Flag-Zbtb38 activated the 4.8 kb RR in a dose-dependent manner in HEK293T cells, whereas knockdown of *Zbtb38* suppressed the activation of 4.8 kb RR in C2C12 cells (Supplementary Figure 4). The rat Zbtb38 homolog, ZENON, has been shown to directly binds to the E-box motif in the tyrosine hydroxylase promoter to activate its transcription[35]. Since two E-box motifs (E1 and E2) were identified within the enhancer regions c and d, respectively (Figure 4C), it suggests that Zbtb38 activates *XIAP* through these motifs. To test this, we constructed luciferase vectors containing mutated E-boxes (E1 mutant: m1; E1 and E2 mutant: m1/m2) within the 4.7 kb RR (Figure 4C). Luciferase assay results showed that overexpression of Zbtb38 activated the wild-type RR, with reduced activation in the m1 mutant and further decreased activation in the m1/m2 mutant (Figure 4D). These results demonstrate that Zbtb38 activates *XIAP* transcription through the E-boxes in enhancers.

We next investigate which domains of Zbtb38 are responsible for activating *XIAP* transcription. A luciferase assay showed that both full-length Zbtb38 and the N-terminal mutant activated the 4.7 kb RR compared to the Flag tag alone (Figure 4E). In contrast, Zbtb38 mutants lacking ZF1-5 showed a loss of activation, suggesting that ZF1-5 is required for activation. To further confirm this, we transfected Zbtb38 and a mutant lacking ZF1-5 (ΔZF1-5) into C2C12 cells and induced

apoptosis by serum deprivation (Figure 4F). The results showed that Myc-Zbtb38 overexpression led to increased XIAP expression and inhibition of apoptosis compared to Myc tag alone, whereas these effects were attenuated in cells transfected with ΔZF1-5 (Supplementary Figure 5). Taken together, these results indicate that ZF1-5 is essential for Zbtb38 to activate XIAP expression and inhibit apoptosis.

Downregulation of XIAP and Bcl-2 by Zbtb38 loss is associated with increased apoptosis during ES cell differentiation and embryogenesis

We have previously shown that loss of Zbtb38 in undifferentiated ES cells does not induce apoptosis but reduces proliferation, suggesting that Zbtb38-depleted cells are more susceptible to apoptosis upon differentiation[30]. To test this possibility, ES cells were cultured in differentiation medium to induce differentiation (Figure 5A). qRT-PCR data showed that the expression of ectodermal genes (*Sox2* and *Nestin*), endodermal genes (*Gata4* and *Gata6*), and mesodermal genes (*Brachyury* and *Mesp1*) were upregulated from day 2 to day 5, indicating that ES cells were undergoing differentiation (Supplementary Figure 6). Immunoblotting results demonstrated that loss of Zbtb38 did not increase the expression of cCasp3 and cPARP compared to the wild-type control on day 0 (Figure 5B-5C). However, loss of Zbtb38 resulted in decreased expression of XIAP (day 0 to day 2) and Bcl-2 (day 0 to day 4), accompanied by increased apoptosis from day 2 to day 5 (Figure 5C). qRT-PCR analysis confirmed that deletion of Zbtb38 led to reduced expression of *XIAP* (d day 0 to day 2) and *Bcl-2* (day 0) compared to their controls (Figure 5D). Unexpectedly, downregulation of *cIAP1*, *cIAP2* and *Bcl-w* was also observed in *Zbtb38*-depleted cells, which may be attributed to the characteristics of ES cells and the complete deletion of *Zbtb38* (Figure 5D, Supplementary Figure 7). In contrast, the expression of other apoptosis-related genes was not significantly altered on day 0 (Supplementary Figure 7). The decreased expression of *cIAP-1, cIAP-2* and *Bcl-w* in *Zbtb38* KO cells may be due to Taken together, these findings suggest that the downregulation of *XIAP* and *Bcl-2* by loss of Zbtb38 in undifferentiated ES cells is a prerequisite for increased apoptosis during ES cell differentiation.

Our previous results demonstrated that heterozygous loss of Zbtb38 resulted in increased apoptosis in E7.5 fetuses [34], a phenomenon that was further investigated using the TUNEL assay, which detects fragmented DNA characteristic of apoptotic cells (Figure 5E). The results revealed a significant increase in the number of TUNEL-positive nuclei in *Zbtb38 Δfl/+* fetuses, contributing to the smaller size of *Zbtb38 Δfl/+* fetuses compared to that of the control (Figure 5F). qRT-PCR analysis showed a reduction in *XIAP* and *Bcl-2* levels in *Δfl/+* embryos compared to controls, whereas the expression of *cIAP1* and *cIAP2* was not reduced (Figure 5G). These results suggest that reduced expression of *XIAP* and *Bcl-2* is a prerequisite for increased apoptosis due to Zbtb38 loss during embryonic development.

In conclusion, our study provides evidence that Zbtb38-associated apoptosis is mediated by direct regulation of *XIAP* expression in differentiated cells, including cancer cells, independent of p53 expression (Figure 6). In comparison, decreased expression of both XIAP and Bcl2 due to Zbtb38 loss contributes to increased apoptosis during ES cell differentiation and embryonic development (Figure

5H). To our knowledge, this is the first report highlighting the importance of E-box motifs in the enhancer region for *XIAP* transcription. The molecular mechanism by which Zbtb38 regulates apoptosis provides a comprehensive understanding of apoptosis, both *in vitro* and *in vivo*, and may potentially pave the way for the development of therapeutic strategies targeting aberrant apoptotic pathways in disease, particularly cancer.

Discussion

This study identified Zbtb38 as a novel regulator of XIAP, a potent suppressor of apoptosis that inhibits the apoptotic cascade and promotes cell survival. Given the role of XIAP in directly inhibiting caspase activity, its transcription is tightly regulated at multiple levels in various cell types. Our data demonstrate that *Zbtb38* knockdown led to decreased *XIAP* expression and increased apoptosis, while Zbtb38 overexpression resulted in increased *XIAP* expression and decreased apoptosis, independent of p53 expression. Furthermore, XIAP overexpression rescued the apoptosis induced by *Zbtb38* knockdown, indicating that Zbtb38-associated apoptosis is at least partially dependent on XIAP expression.

Undifferentiated mouse ES cells typically exhibit a faster replication rate and greater resistance to apoptosis compared to differentiated cells[36][37]. Consistent with this, our previous findings and this study showed that loss of *Zbtb38* (KD or KO) in undifferentiated ES cells does not induce apoptosis during proliferation[30]. However, our previous data revealed that in Zbtb38 KO ES cells, Nanog, key for proliferation, was downregulated, while Oct4 and Sox2, key for self-renewal, were unaffected, suggesting that Zbtb38-depleted cells are more prone to apoptosis upon differentiation[38][39]. In this study, we found that loss of Zbtb38 in undifferentiated ES cells decreased XIAP and Bcl-2 expression, which may account for the increased apoptosis observed during differentiation. In addition, reduced *Bcl-2* expression was found in *Zbtb38* heterozygous KO E7.5 embryos and in some *Zbtb38* knockdown cells (NMuMG and C2C12), suggesting that downregulation of both XIAP and Bcl-2 is a prerequisite for Zbtb38 loss-induced apoptosis during these processes. Collectively, our findings highlight the importance of the Zbtb38-XIAP/Bcl2 axis in ES cell differentiation and early embryogenesis, underscoring its role in preventing unnecessary apoptosis, which may have implications for developmental biology and regenerative medicine.

In this study, ChIP and luciferase assays showed that Zbtb38 directly regulates *XIAP* transcription via E-box motifs in the *XIAP* enhancers. Luciferase assay and immunoblotting data demonstrated that the ZF1-5 domain of Zbtb38 is essential for the activation of XIAP transcription and inhibition of apoptosis. The presence of an E-box motif in the Bcl-2 promoter suggests that Zbtb38 also directly regulates Bcl-2 transcription via the E-box, although further experiments are needed to confirm this [40]. E-box is a well-known regulatory element crucial for the regulation of gene expression, recruitment of transcription factors, such as basic helix-loop-helix proteins, and chromatin remodeling[41]. E-box functions are essential for development, cellular responses to environmental cues, and various diseases, including cancer and neurodevelopmental disorders[42]. Since the E-boxes in the *XIAP* enhancer are critical for Zbtb38-mediated *XIAP* transcription, chemicals that inhibit this binding are expected to decrease *XIAP* expression and increase apoptosis in cancer cells.

XIAP is often overexpressed in cancer, promoting tumor progression and resistance to chemotherapy and radiotherapy[43]. High XIAP levels are associated with poor prognosis and survival in many cancers[44]. Consequently, inhibition of XIAP using small molecule inhibitors and antisense oligonucleotides has been shown to overcome resistance to apoptosis in cancer therapy

[45][46][47][47]. Zbtb38 has been reported to be highly expressed in bladder cancer and may promote the migration and invasive growth of these cancer cells[48], suggesting a potential link between Zbtb38 expression and cancer. Notably, both XIAP and Zbtb38 are ubiquitously expressed in various cell types and tissues[16][25]. Using the Cancer Genomics database (https://www.cbioportal.org/), we found a correlation between high copy number amplification of *Zbtb38* and *XIAP* in several cancer cell lines, including bladder urothelial carcinoma, cervical squamous cell carcinoma, esophageal adenocarcinoma, head and neck squamous cell carcinoma, and ovarian serous cystadenocarcinoma (data not shown). In addition, some human cancers overexpress both Bcl-2 and XIAP to escape apoptosis, and the combined inhibition of XIAP and BCL2 has been shown to provide maximal therapeutic efficacy in aggressive cancers, such as acute myeloid leukemia[49]. Future studies are needed to investigate the apoptotic status after *Zbtb38* inhibition in these cancer cells.

p53 is a potent regulator of apoptosis, but is inactivated in approximately 50% of cancers, leading to chemotherapy resistance and reduced therapeutic efficacy[15][50]. Therefore, inducing apoptosis independent of p53 expression is a promising strategy for treating p53-deficient cancers[51][52]. In this study, we found that apoptosis induced by Zbtb38 loss depends on XIAP, but not on p53 expression, in both normal and cancer cells. Thus, inhibition of the Zbtb38-XIAP pathway may be a useful therapeutic approach for cancers with p53 dysfunction, although further validation in more p53-deficient cancer cell lines is required.

Zbtb38 is a methyl-CpG-binding protein that binds methylated CpG via its ZF1-5 domain and represses its targets via its N-terminal domains[25][28][53]. This study demonstrate that Zbtb38-associated apoptosis is mediated by a DNA methylation-independent mechanism, in addition to its canonical role as a methyl-CpG-binding protein. Our data indicate that the ZF1-5 domain is essential for Zbtb38 binding to the E-box and activating *XIAP* transcription, similar to Zbtb33/Kaiso, where the Kaiso zinc fingers are required for binding to both non-methylated and methylated sequences[54]. Genome-wide association studies in humans have identified the ZBTB38 gene as most strongly associated with height, with a single nucleotide polymorphism at rs6763931 being highly correlated with its expression in the blood[55]. Zbtb38 is ubiquitously expressed in tissues, and its expression is associated with various diseases, including cancer[56–59] and neurodegenerative diseases[60][59]. Our findings suggest that the non-methylated and/or methylated mechanisms of Zbtb38 may contribute to its physiological functions and explain its role in these diseases, adding complexity to its role in epigenetic regulation.

In conclusion, our study provides evidence that Zbtb38 plays a critical role in apoptosis by regulating XIAP and/or Bcl-2 expression in both undifferentiated and differentiated cells, including a cancer cell line, independently of p53 and DNA methylation. The mechanisms underlying Zbtb38-mediated apoptosis may serve as a basis for further developmental research and potentially novel therapeutic approaches for diseases, particularly cancer.

Figure Legends

Figure 1. Expression of apoptosis-related genes after *Zbtb38* knockdown in p53-expressing (MEFs, NMuMG and C2C12) and p53-deficient (*p53* KO, 4T1 and DKO) cells.

The mRNA levels of the indicated genes in the negative control (NC, empty column) and *Zbtb38* knockdown (KD, gray column) groups were determined by qRT-PCR. The GAPDH gene was used as an internal control, and the levels of the transcripts were normalized to the GAPDH gene, which was designated as "1". $*p < 0.05$, $**p < 0.01$, $***p < 0.001$. "ns" indicates no significance.

Figure 2. siRNA-mediated knockdown of *Zbtb38* in p53-expressing and p53-deficient cells.

2A-2D. siRNA duplex was used to downregulate Zbtb38 expression in MEFs (**2A**), *p53* KO MEFs (**2B**), NMuMG cells (**2C**), and 4T1 cells (**2D**). The expression of Zbtb38, XIAP, cPARP, and cCasp3 was detected with the corresponding antibodies. GAPDH was used as an internal control for immunoblotting. Data were quantified relative to GAPDH, which is shown in the lower panel of each immunoblot. Negative control (NC, empty column), *Zbtb38* knockdown (KD, grey column). $*p < 0.05$.

Figure 3. Zbtb38 overexpression inhibits apoptosis and increases XIAP expression.

3A, C2C12 cells were transfected with Flag or Flag-Zbtb38 for 36 h, then switched to medium without FBS (0% serum) for 1 h. **3B-3C**, *p53* KO MEFs were transfected with Flag or Flag-Zbtb38 for 30–36 h, then switched to medium lacking FBS for 1h (**3B)** or treated with 0.4 mM H_2O_2 for 1h (**3C**). **3D-3E**, overexpressed XIAP rescued apoptosis induced by *Zbtb38* knockdown in C2C12 cells (**3D**) and *p53* KO MEFs (**3E**). *p53* KO MEFs or C2C12 cells were transfected with siRNA against *Zbtb38* or a negative control (-) for 24 h, followed by transfection with increased XIAP for 24 h (**3D**), or XIAP or Flag-XIAP for 24 h (**3E**). F-X: Flag-XIAP. Arrows indicate wild-type or endogenous (endo) and exogenous (exo) XIAP (**3E**). **3A-3E,** data were quantified relative to GAPDH, and quantification results are shown in the lower panel of each immunoblot. $*p < 0.05$, $***p < 0.001$.

Figure 4. Zbtb38 directly activates *XIAP* transcription via E-boxes.

4A, schematic of *XIAP* regulatory regions (upper panel); red circles represent the conserved regions among vertebrate species. Regions a and b represent putative promoter regions, and regions c and d indicate enhancer regions. *TSS*, transcriptional start site. **4B,** ChIP-qPCR results for C2C12 cells. IgG-precipitated DNA (negative control) and Zbtb38-immunoprecipitated DNA were amplified by qRT-PCR using primers at the indicated locations. Data are shown as fold enrichment relative to the input control, which was set to 1. **4C,** schematic representation of two conserved E-box motifs in the *XIAP* regulatory region. wt: wild-type E-box, m1: E-box1 mutant, m1m2: E-box1 and E-box2 mutant. The underlined sequences represent nucleotide changes relative to the wild type. *Luc*, luciferase reporter. **4D,** pGL3, or the indicated pGL3 plasmid DNA was co-transfected with Flag or Flag-Zbtb38 into HEK293T cells. Luciferase activity was determined relative to that of pGL3/Flag, which was normalized to 1. **4E,** schematic representation of Zbtb38 deletion mutants fused to Flag and their activation activity in pGL3-XIAP. Luciferase activity was determined relative to that of

pGL3/Flag, which was normalized to 1. **4B-4E,** *$p < 0.05$, **$p < 0.01$, ***$p < 0.001$. "ns" indicates no significance.

Figure 5. Decreased expression of XIAP and Bcl-2 is responsible for the apoptosis induced by Zbtb38 loss during ES cell differentiation and embryogenesis.

5A, schematic of the ES cell differentiation assay. ES cells were cultured in ES medium to maintain an undifferentiated state (d0) and then differentiated into embryoid bodies (EBs) in suspension culture lacking LIF. **5B-5C,** immunoblotting of the indicated proteins in wild-type (WT) and *Zbtb38* knockout (KO) ES cells at different differentiation days. Protein levels were detected with specific antibodies (**5B**) and quantified relative to GAPDH, indicated as "1" relative to WT at d0 (**5C**). Wild-type (WT, blank column), *Zbtb38* KO (KO, gray column). **5D,** qRT-PCR of gene expression in WT and *Zbtb38* KO ES cells at the indicated differentiation days. Each transcript level was quantified relative to *that of GAPDH*. **5E,** schematic of the strategy for generating *fl/+* and Δ*fl/+* fetuses, and a photograph of E7.5 fetuses. *fl* denotes *flox*. Scale bar: 100 μm. **5F,** 5F: TUNEL assay on paraffin-embedded E7.5 embryo sections. TUNEL-positive cells are shown in green, and nuclei were counterstained with PI (red). Scale bar: 100 μm. Quantitative analysis of TUNEL-positive cells relative to PI-positive nuclei is shown on the right. *fl/+* (n = 5), *Δfl/+* (n = 5). **5G,** qRT-PCR of *Zbtb38* and apoptosis markers in E7.5 fetuses. Each transcript level was quantified relative to *that of GAPDH*. *fl/+* (n = 3), and Δ*fl/+* (n = 3) embryos. **5C-5G,** *$p < 0.05$, **$p < 0.01$, ***$p < 0.001$. ns" indicates no significant difference.

Figure 6. schematic model of the Zbtb38-XIAP or Zbtb38-XIAP/Bcl-2 axis in the regulation of apoptosis.

ACKNOWLEDGMENT

We would like to thank Drs. Chio Oka and Masashi Kawaichi for their valuable suggestions and discussions. We also thank Mr. Shunya Hibia and Mr. Ibuki Okuda for their technical support, as well as the members of the Ishida laboratory for their suggestions and technical advice. This work was supported by a Grant-in-Aid for Scientific Research (16K08587) from the Japan Society for the Promotion of Science (JSPS).

CONFLICT OF INTEREST

The authors declare no conflicts of interest.

CONTRIBUTIONS

N.H. and S.T. conceived, designed, performed the experiments, and analyzed the data. T.S. planned the study, conceived the project, and provided technical guidance and helpful conceptual advice. E.M. conceived, designed, performed the experiments, analyzed the data, prepared the figures, and drafted the manuscript. N.N., Y.I., and Y.B. supervised the work and approved the manuscript.

DATA AVALILABILITY

The data used to support the findings of this study are available from the corresponding author upon reasonable request.

References

1. Elmore, S. Apoptosis: A Review of Programmed Cell Death. *Toxicol Pathol* 2007, *35*.
2. Obeng, E. Apoptosis (Programmed Cell Death) and Its Signals-a Review. *Brazilian Journal of Biology* 2021, *81*.
3. Nagata, S. Apoptosis and Clearance of Apoptotic Cells. *Annu Rev Immunol* **2018**, *36*, 489–517, doi:10.1146/annurev-immunol-042617-053010.
4. Bock, F.J.; Tait, S.W.G. Mitochondria as Multifaceted Regulators of Cell Death. *Nat Rev Mol Cell Biol* 2020, *21*, 85–100.
5. Lossi, L. The Concept of Intrinsic versus Extrinsic Apoptosis. *Biochemical Journal* 2022, *479*.
6. Larsen, B.D.; Sørensen, C.S. The Caspase - activated <scp>DN</Scp> Ase: Apoptosis and Beyond. *FEBS J* **2017**, *284*, 1160–1170, doi:10.1111/febs.13970.
7. Sahoo, G.; Samal, D.; Khandayataray, P.; Murthy, M.K. A Review on Caspases: Key Regulators of Biological Activities and Apoptosis. *Mol Neurobiol* 2023, *60*.
8. Soldani, C.; Lazzè, M.C.; Bottone, M.G.; Tognon, G.; Biggiogera, M.; Pellicciari, C.E.; Scovassi, A.I. Poly(ADP-Ribose) Polymerase Cleavage during Apoptosis: When and Where? *Exp Cell Res* **2001**, *269*, doi:10.1006/excr.2001.5293.
9. Czabotar, P.E.; Garcia-Saez, A.J. Mechanisms of BCL-2 Family Proteins in Mitochondrial Apoptosis. *Nat Rev Mol Cell Biol* 2023, *24*.
10. Siddiqui, W.A.; Ahad, A.; Ahsan, H. The Mystery of BCL2 Family: Bcl-2 Proteins and Apoptosis: An Update. *Arch Toxicol* 2015, *89*, 289–317.
11. Kale, J.; Osterlund, E.J.; Andrews, D.W. BCL-2 Family Proteins: Changing Partners in the Dance towards Death. *Cell Death Differ* 2018, *25*.
12. Joza, N.; Susin, S.A.; Daugas, E.; Stanford, W.L.; Cho, S.K.; Li, C.Y.J.; Sasaki, T.; Elia, A.J.; Cheng, H.Y.M.; Ravagnan, L.; et al. Essential Role of the Mitochondrial Apoptosis-Inducing Factor in Programmed Cell Death. *Nature* **2001**, *410*, doi:10.1038/35069004.
13. Alam, M.; Ali, S.; Mohammad, T.; Hasan, G.M.; Yadav, D.K.; Hassan, M.I. B Cell Lymphoma 2: A Potential Therapeutic Target for Cancer Therapy. *Int J Mol Sci* 2021, *22*.
14. Hao, Q.; Chen, J.; Lu, H.; Zhou, X. The ARTS of P53-Dependent Mitochondrial Apoptosis. *J Mol Cell Biol* **2022**, *14*, doi:10.1093/jmcb/mjac074.
15. Aubrey, B.J.; Kelly, G.L.; Janic, A.; Herold, M.J.; Strasser, A. How Does P53 Induce Apoptosis and How Does This Relate to P53-Mediated Tumour Suppression? *Cell Death Differ* 2018, *25*.
16. Liston, P.; Young, S.S.; Mackenzie, A.E.; Korneluk, R.G. Life and Death Decisions: The Role of the IAPs in Modulating Programmed Cell Death. *Apoptosis* **1997**, *2*, doi:10.1023/A:1026465926478.
17. Deveraux, Q.L.; Reed, J.C. IAP Family Proteins - Suppressors of Apoptosis. *Genes Dev* 1999, *13*.
18. Dohi, T.; Okada, K.; Xia, F.; Wilford, C.E.; Samuel, T.; Welsh, K.; Marusawa, H.; Zou, H.; Armstrong, R.; Matsuzawa, S.I.; et al. An IAP-IAP Complex Inhibits Apoptosis. *Journal of*

Biological Chemistry **2004**, *279*, 34087–34090, doi:10.1074/jbc.C400236200.

19. Dubrez-Daloz, L.; Dupoux, A.; Cartier, J. IAPs: More than Just Inhibitors of Apoptosis Proteins. *Cell Cycle* 2008, *7*.
20. Harlin, H.; Reffey, S.B.; Duckett, C.S.; Lindsten, T.; Thompson, C.B. Characterization of XIAP-Deficient Mice. *Mol Cell Biol* **2001**, *21*, doi:10.1128/mcb.21.10.3604-3608.2001.
21. Moulin, M.; Anderton, H.; Voss, A.K.; Thomas, T.; Wong, W.W.L.; Bankovacki, A.; Feltham, R.; Chau, D.; Cook, W.D.; Silke, J.; et al. IAPs Limit Activation of RIP Kinases by TNF Receptor 1 during Development. *EMBO Journal* **2012**, *31*, doi:10.1038/emboj.2012.18.
22. Heard, K.N.; Bertrand, M.J.; Barker, P.A. CIAP2 Supports Viability of Mice Lacking CIAP1 and XIAP. *EMBO J* **2015**, *34*, doi:10.15252/embj.201592060.
23. Dynek, J.N.; Vucic, D. Antagonists of IAP Proteins as Cancer Therapeutics. *Cancer Lett* 2013, *332*.
24. Verhagen, A.M.; Silke, J.; Ekert, P.G.; Pakusch, M.; Kaufmann, H.; Connolly, L.M.; Day, C.L.; Tikoo, A.; Burke, R.; Wrobel, C.; et al. HtrA2 Promotes Cell Death through Its Serine Protease Activity and Its Ability to Antagonize Inhibitor of Apoptosis Proteins. *Journal of Biological Chemistry* **2002**, *277*, doi:10.1074/jbc.M109891200.
25. Sasai, N.; Matsuda, E.; Sarashina, E.; Ishida, Y.; Kawaichi, M. Identification of a Novel BTB-Zinc Finger Transcriptional Repressor, CIBZ, That Interacts with CtBP Corepressor. *Genes to Cells* **2005**, *10*, doi:10.1111/j.1365-2443.2005.00885.x.
26. Filion, G.J.P.; Zhenilo, S.; Salozhin, S.; Yamada, D.; Prokhortchouk, E.; Defossez, P.-A. A Family of Human Zinc Finger Proteins That Bind Methylated DNA and Repress Transcription. *Mol Cell Biol* **2006**, *26*, 169–181, doi:10.1128/mcb.26.1.169-181.2006.
27. Sasai, N.; Nakao, M.; Defossez, P.A. Sequence-Specific Recognition of Methylated DNA by Human Zinc-Finger Proteins. *Nucleic Acids Res* **2010**, *38*, 5015–5022, doi:10.1093/nar/gkq280.
28. Oikawa, Y.; Omori, R.; Nishii, T.; Ishida, Y.; Kawaichi, M.; Matsuda, E. The Methyl-CpG-Binding Protein CIBZ Suppresses Myogenic Differentiation by Directly Inhibiting Myogenin Expression. *Cell Res* **2011**, *21*, 1578–1590, doi:10.1038/cr.2011.90.
29. de Dieuleveult, M.; Miotto, B. DNA Methylation and Chromatin: Role(s) of Methyl-CpG-Binding Protein ZBTB38. *Epigenet Insights* 2018, *11*.
30. Nishii, T.; Oikawa, Y.; Ishida, Y.; Kawaichi, M.; Matsuda, E. CtBP-Interacting BTB Zinc Finger Protein (CIBZ) Promotes Proliferation and G1/S Transition in Embryonic Stem Cells via Nanog. *Journal of Biological Chemistry* **2012**, *287*, doi:10.1074/jbc.M111.333856.
31. Kotoku, T.; Kosaka, K.; Nishio, M.; Ishida, Y.; Kawaichi, M.; Matsuda, E. CIBZ Regulates Mesodermal and Cardiac Differentiation of by Suppressing T and Mesp1 Expression in Mouse Embryonic Stem Cells. *Sci Rep* **2016**, *6*, 34188, doi:10.1038/srep34188.
32. Oikawa, Y.; Matsuda, E.; Nishii, T.; Ishida, Y.; Kawaichi, M. Down-Regulation of CIBZ, a Novel Substrate of Caspase-3, Induces Apoptosis. *Journal of Biological Chemistry* **2008**, *283*, doi:10.1074/jbc.M802257200.

33. Cai, Y.; Li, J.; Zhang, Z.; Chen, J.; Zhu, Y.; Li, R.; Chen, J.; Gao, L.; Liu, R.; Teng, Y. Zbtb38 Is a Novel Target for Spinal Cord Injury. *Oncotarget* **2017**, *8*, 45356–45366, doi:10.18632/oncotarget.17487.
34. Nishio, M.; Matsuura, T.; Hibi, S.; Ohta, S.; Oka, C.; Sasai, N.; Ishida, Y.; Matsuda, E. Heterozygous Loss of Zbtb38 Leads to Early Embryonic Lethality via the Suppression of Nanog and Sox2 Expression. *Cell Prolif* **2022**, *55*, doi:10.1111/cpr.13215.
35. Kiefer, H.; Chatail-Hermitte, F.; Ravassard, P.; Bayard, E.; Brunet, I.; Mallet, J. ZENON, a Novel POZ Kruppel-Like DNA Binding Protein Associated with Differentiation and/or Survival of Late Postmitotic Neurons. *Mol Cell Biol* **2005**, *25*, 1713–1729, doi:10.1128/mcb.25.5.1713-1729.2005.
36. Ying, Q.L.; Wray, J.; Nichols, J.; Batlle-Morera, L.; Doble, B.; Woodgett, J.; Cohen, P.; Smith, A. The Ground State of Embryonic Stem Cell Self-Renewal. *Nature* **2008**, *453*, doi:10.1038/nature06968.
37. Vouzas, A.E.; Gilbert, D.M. Mammalian DNA Replication Timing. *Cold Spring Harb Perspect Biol* **2021**, *13*, doi:10.1101/cshperspect.a040162.
38. Chambers, I.; Tomlinson, S.R. The Transcriptional Foundation of Pluripotency. *Development* 2009, *136*.
39. Strebinger, D.; Deluz, C.; Friman, E.T.; Govindan, S.; Alber, A.B.; Suter, D.M. Endogenous Fluctuations of OCT 4 and SOX 2 Bias Pluripotent Cell Fate Decisions . *Mol Syst Biol* **2019**, *15*, doi:10.15252/msb.20199002.
40. McGill, G.G.; Horstmann, M.; Widlund, H.R.; Du, J.; Motyckova, G.; Nishimura, E.K.; Lin, Y.L.; Ramaswamy, S.; Avery, W.; Ding, H.F.; et al. Bcl2 Regulation by the Melanocyte Master Regulator Mitf Modulates Lineage Survival and Melanoma Cell Viability. *Cell* **2002**, *109*, doi:10.1016/S0092-8674(02)00762-6.
41. Michael, A.K.; Stoos, L.; Crosby, P.; Eggers, N.; Nie, X.Y.; Makasheva, K.; Minnich, M.; Healy, K.L.; Weiss, J.; Kempf, G.; et al. Cooperation between BHLH Transcription Factors and Histones for DNA Access. *Nature* **2023**, *619*, 385–393, doi:10.1038/s41586-023-06282-3.
42. Pan, Y.; van der Watt, P.J.; Kay, S.A. E-Box Binding Transcription Factors in Cancer. *Front Oncol* 2023, *13*.
43. Tu, H.; Costa, M. Xiap's Profile in Human Cancer. *Biomolecules* 2020, *10*.
44. Gao, X.; Zhang, L.; Wei, Y.; Yang, Y.; Li, J.; Wu, H.; Yin, Y. Prognostic Value of XIAP Level in Patients with Various Cancers: A Systematic Review and Meta-Analysis. *J Cancer* **2019**, *10*, doi:10.7150/jca.28229.
45. Holcik, M.; Gibson, H.; Korneluk, R.G. XIAP: Apoptotic Brake and Promising Therapeutic Target. *Apoptosis* 2001, *6*, 253–261.
46. Oost, T.K.; Sun, C.; Armstrong, R.C.; Al-Assaad, A.S.; Betz, S.F.; Deckwerth, T.L.; Ding, H.; Elmore, S.W.; Meadows, R.P.; Olejniczak, E.T.; et al. Discovery of Potent Antagonists of the Antiapoptotic Protein XIAP for the Treatment of Cancer. *J Med Chem* **2004**, *47*,

doi:10.1021/jm040037k.

47. Schimmer, A.D.; Welsh, K.; Pinilla, C.; Wang, Z.; Krajewska, M.; Bonneau, M.J.; Pedersen, I.M.; Kitada, S.; Scott, F.L.; Bailly-Maitre, B.; et al. Small-Molecule Antagonists of Apoptosis Suppressor XIAP Exhibit Broad Antitumor Activity. *Cancer Cell* **2004**, *5*, doi:10.1016/S1535-6108(03)00332-5.
48. Jing, J.; Liu, J.; Wang, Y.; Zhang, M.; Yang, L.; Shi, F.; Liu, P.; She, J. The Role of ZBTB38 in Promoting Migration and Invasive Growth of Bladder Cancer Cells. *Oncol Rep* **2019**, *41*, doi:10.3892/or.2018.6937.
49. Hashimoto, M.; Saito, Y.; Nakagawa, R.; Ogahara, I.; Takagi, S.; Takata, S.; Amitani, H.; Endo, M.; Yuki, H.; Ramilowski, J.A.; et al. Combined Inhibition of XIAP and BCL2 Drives Maximal Therapeutic Efficacy in Genetically Diverse Aggressive Acute Myeloid Leukemia. *Nat Cancer* **2021**, *2*, doi:10.1038/s43018-021-00177-w.
50. Hassin, O.; Oren, M. Drugging P53 in Cancer: One Protein, Many Targets. *Nat Rev Drug Discov* **2023**, *22*, 127–144, doi:10.1038/s41573-022-00571-8.
51. Speidel, D. Transcription-Independent P53 Apoptosis: An Alternative Route to Death. *Trends Cell Biol* 2010, *20*.
52. Marei, H.E.; Althani, A.; Afifi, N.; Hasan, A.; Caceci, T.; Pozzoli, G.; Morrione, A.; Giordano, A.; Cenciarelli, C. P53 Signaling in Cancer Progression and Therapy. *Cancer Cell Int* 2021, *21*.
53. Marchal, C.; Defossez, P.A.; Miotto, B. Context-Dependent CpG Methylation Directs Cell-Specific Binding of Transcription Factor ZBTB38. *Epigenetics* **2022**, *17*, doi:10.1080/15592294.2022.2111135.
54. Buck-Koehntop, B.A.; Martinez-Yamout, M.A.; Jane Dyson, H.; Wright, P.E. Kaiso Uses All Three Zinc Fingers and Adjacent Sequence Motifs for High Affinity Binding to Sequence-Specific and Methyl-CpG DNA Targets. *FEBS Lett* **2012**, *586*, doi:10.1016/j.febslet.2012.01.045.
55. Gudbjartsson, D.F.; Walters, G.B.; Thorleifsson, G.; Stefansson, H.; Halldorsson, B. V.; Zusmanovich, P.; Sulem, P.; Thorlacius, S.; Gylfason, A.; Steinberg, S.; et al. Many Sequence Variants Affecting Diversity of Adult Human Height. *Nat Genet* **2008**, *40*, 609–615, doi:10.1038/ng.122.
56. Kote-Jarai, Z.; Olama, A.A. Al; Giles, G.G.; Severi, G.; Schleutker, J.; Weischer, M.; Campa, D.; Riboli, E.; Key, T.; Gronberg, H.; et al. Seven Prostate Cancer Susceptibility Loci Identified by a Multi-Stage Genome-Wide Association Study. *Nat Genet* **2011**, *43*, 785–791, doi:10.1038/ng.882.
57. Jing, J.; Liu, J.; Wang, Y.; Zhang, M.; Yang, L.; Shi, F.; Liu, P.; She, J. The Role of ZBTB38 in Promoting Migration and Invasive Growth of Bladder Cancer Cells. *Oncol Rep* **2019**, *41*, 1980–1990, doi:10.3892/or.2018.6937.
58. de Dieuleveult, M.; Marchal, C.; Jouinot, A.; Letessier, A.; Miotto, B. Molecular and Clinical Relevance of ZBTB38 Expression Levels in Prostate Cancer. *Cancers (Basel)* **2020**, *12*, doi:10.3390/cancers12051106.

59. Chen, J.; Xing, C.; Yan, L.; Wang, Y.; Wang, H.; Zhang, Z.; Yu, D.; Li, J.; Li, H.; Li, J.; et al. Transcriptome Profiling Reveals the Role of ZBTB38 Knock-down in Human Neuroblastoma. *PeerJ* **2019**, *7*, e6352, doi:10.7717/peerj.6352.
60. Mead, S.; Uphill, J.; Beck, J.; Poulter, M.; Campbell, T.; Lowe, J.; Adamson, G.; Hummerich, H.; Klopp, N.; Rückert, I.-M.; et al. Genome-Wide Association Study in Multiple Human Prion Diseases Suggests Genetic Risk Factors Additional to PRNP. *Hum Mol Genet* **2012**, *21*, 1897–1906, doi:10.1093/hmg/ddr607.

1

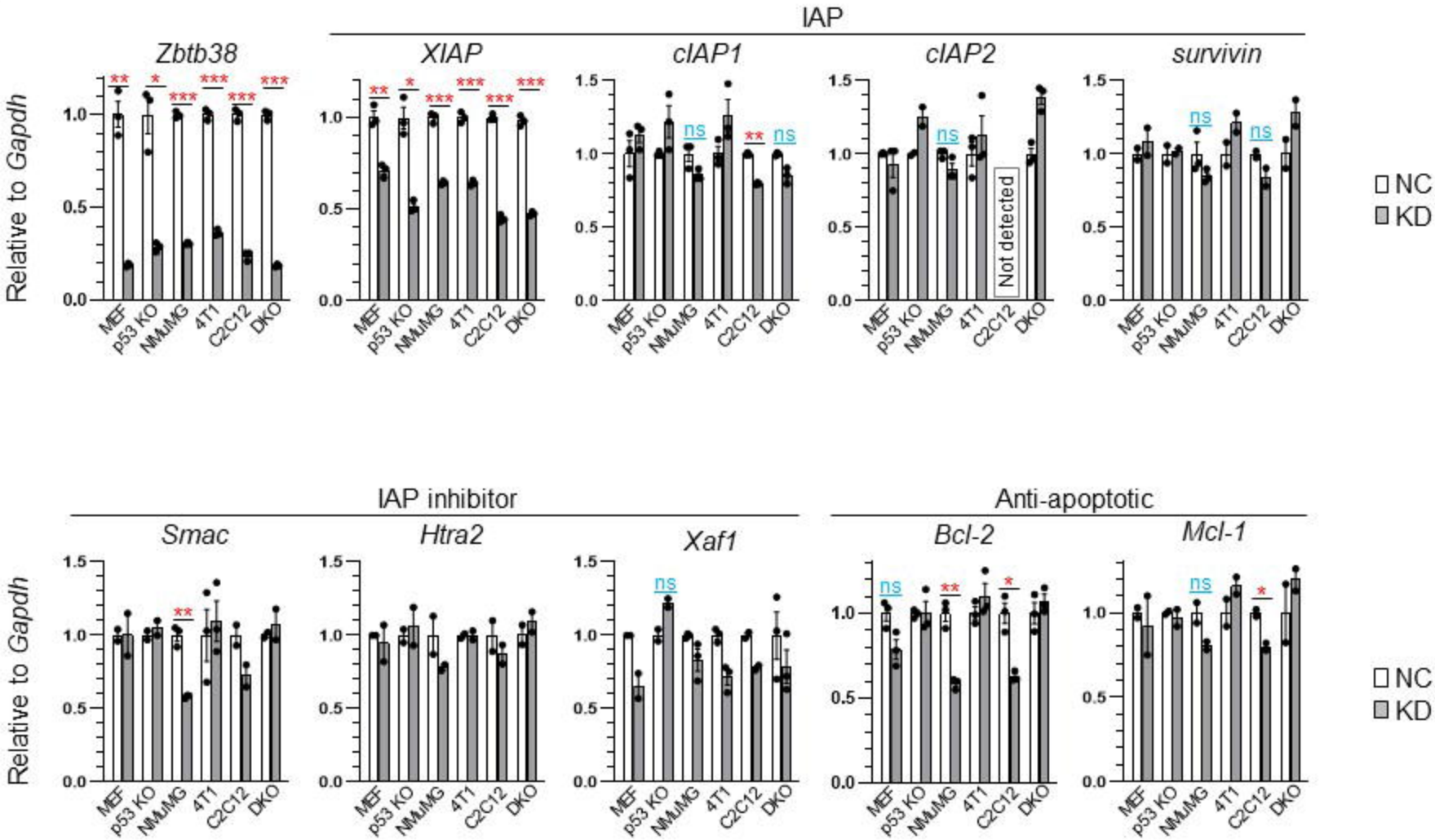
IAP
Zbtb38
XIAP
cIAP1
cIAP2
survivin
Relative to Gapdh
Not detected
NC
KD
IAP inhibitor
Smac
Htra2
Xaf1
Anti-apoptotic
Bcl-2
Mcl-1
MEF
p53 KO
NMuMG
4T1
C2C12
DKO
ns
*
**
***

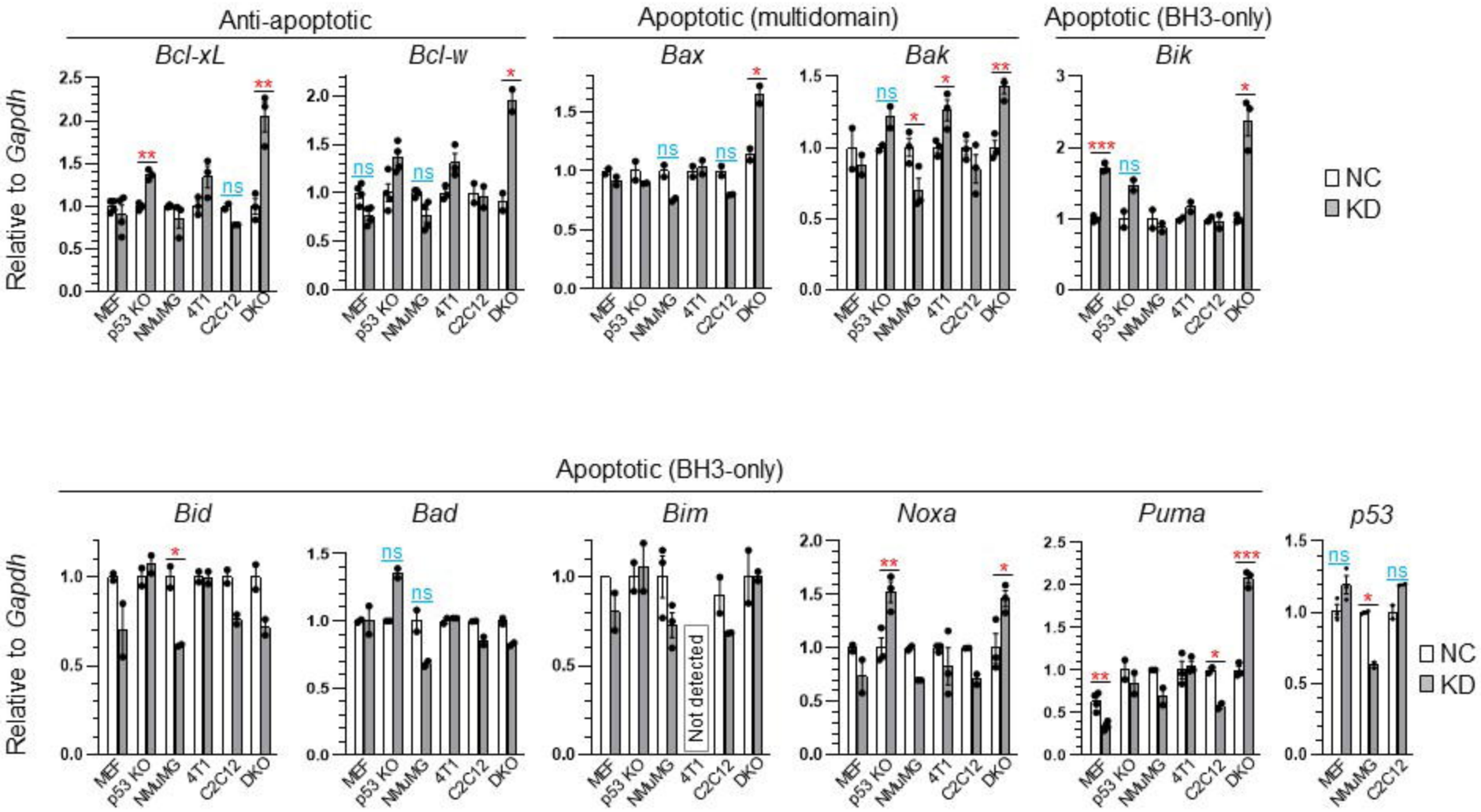
Anti-apoptotic
Apoptotic (multidomain)
Apoptotic (BH3-only)
Bcl-xL
Bcl-w
Bax
Bak
Bik
Relative to Gapdh
MEF
p53 KO
NMuMG
4T1
C2C12
DKO
NC
KD
ns
Apoptotic (BH3-only)
Bid
Bad
Bim
Noxa
Puma
p53
Not detected

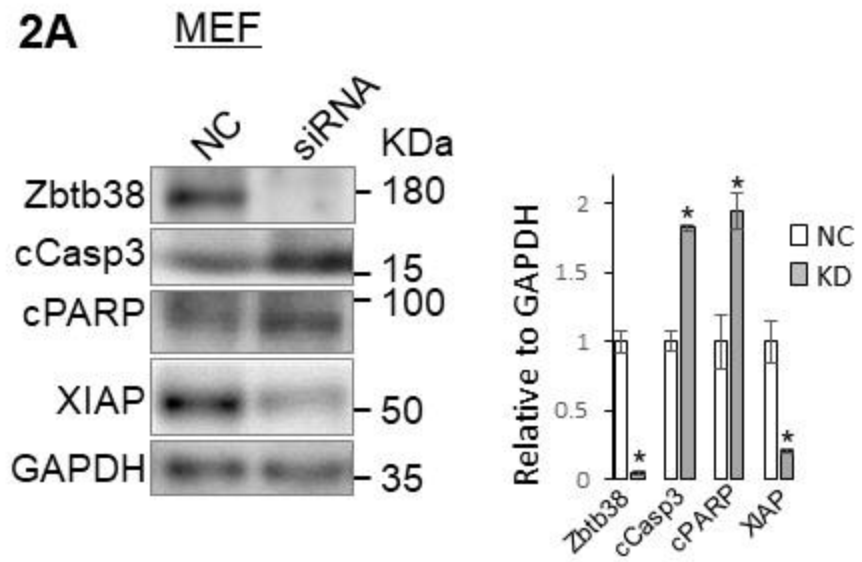
2A
MEF
NC
siRNA
KDa
Zbtb38
cCasp3
cPARP
XIAP
GAPDH
180
15
100
50
35
Relative to GAPDH
NC
KD
Zbtb38
cCasp3
cPARP
XIAP

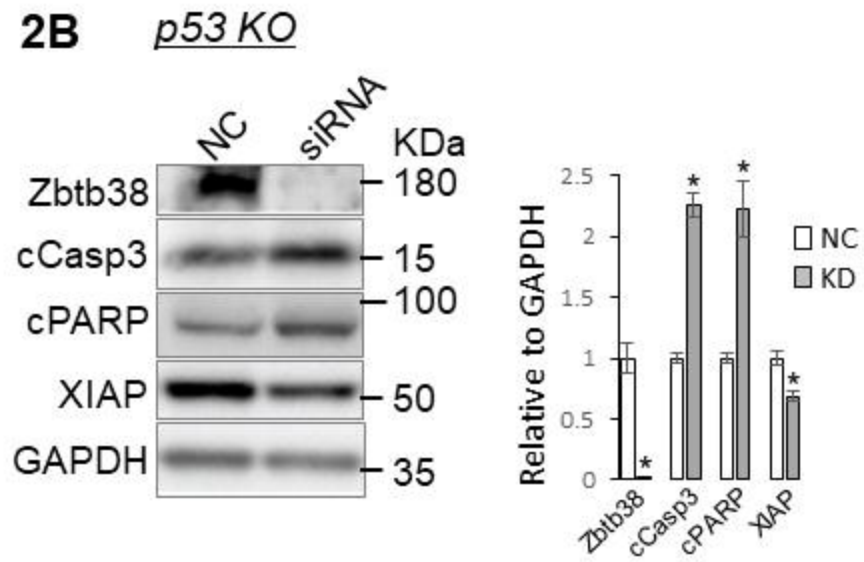
2B
p53 KO
NC
siRNA
KDa
Zbtb38
cCasp3
cPARP
XIAP
GAPDH
180
15
100
50
35
Relative to GAPDH
NC
KD
Zbtb38
cCasp3
cPARP
XIAP

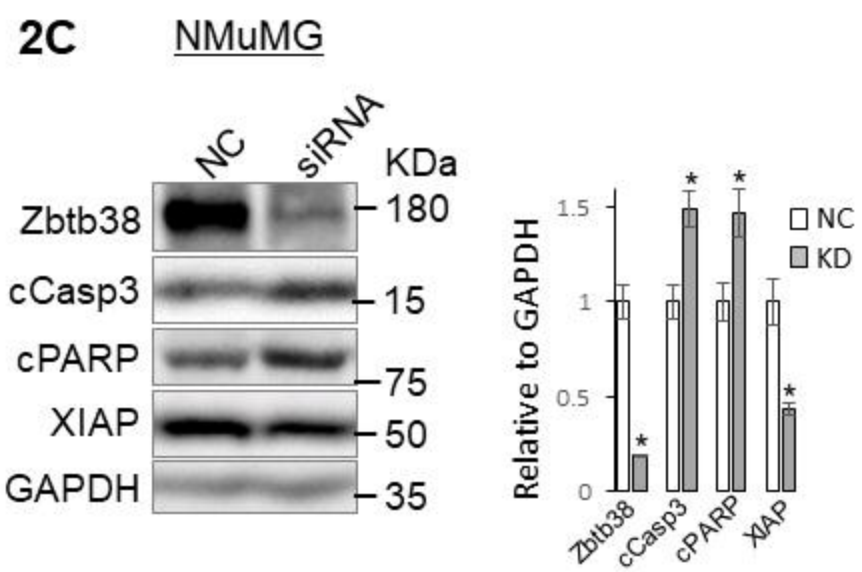
2C
NMuMG
NC
siRNA
KDa
Zbtb38
cCasp3
cPARP
XIAP
GAPDH
180
15
75
50
35
Relative to GAPDH
NC
KD
Zbtb38
cCasp3
cPARP
XIAP

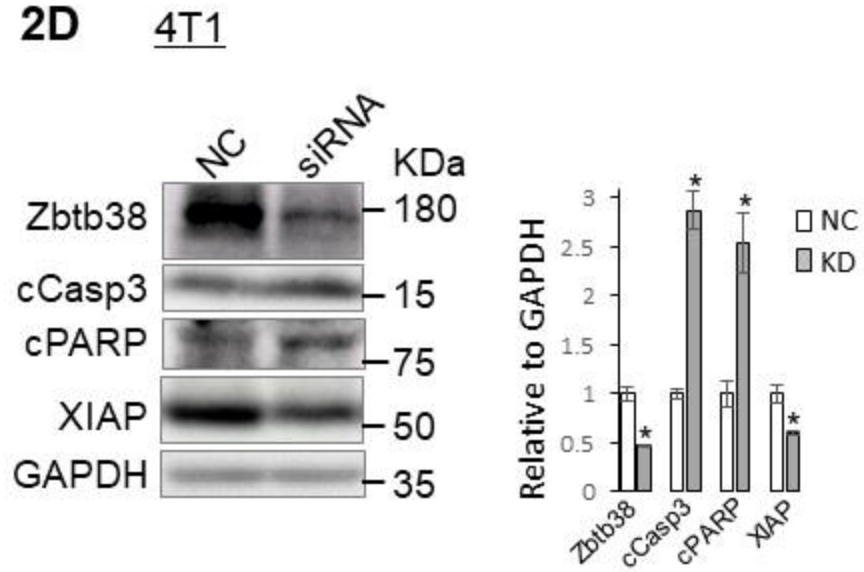
2D
4T1
NC
siRNA
KDa
Zbtb38
cCasp3
cPARP
XIAP
GAPDH
180
15
75
50
35
Relative to GAPDH
NC
KD
Zbtb38
cCasp3
cPARP
XIAP

3A C2C12

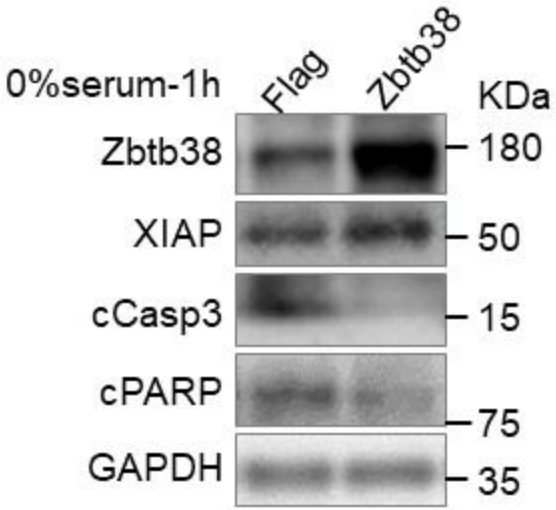

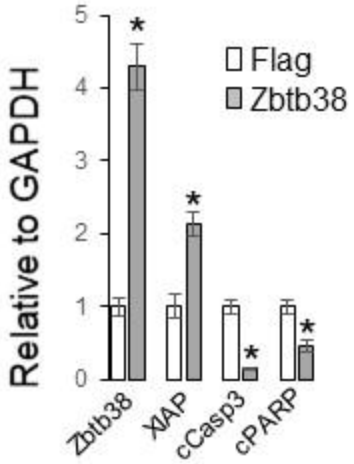

3B *p53 KO*

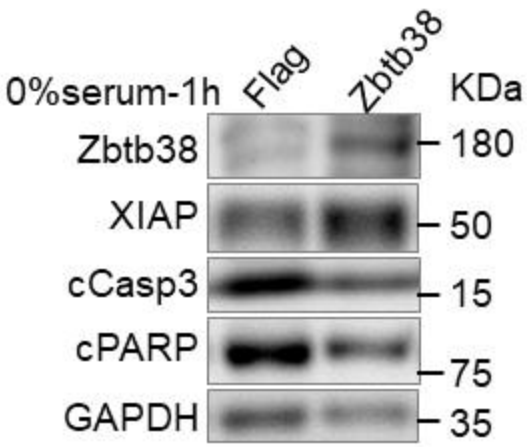

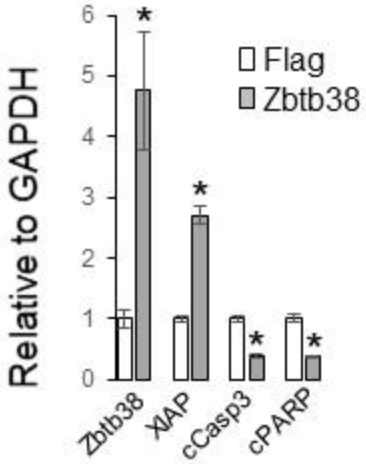

3C *p53 KO*

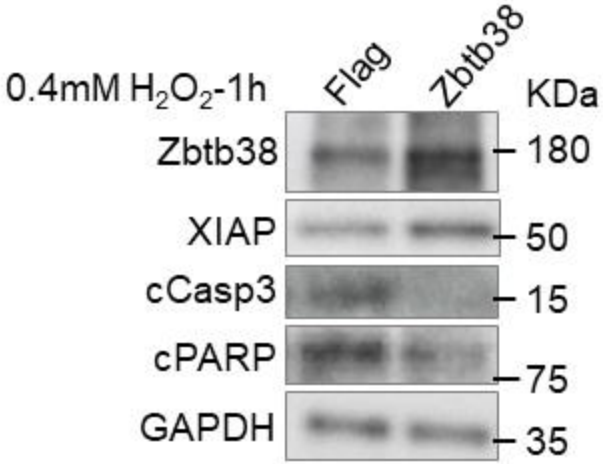

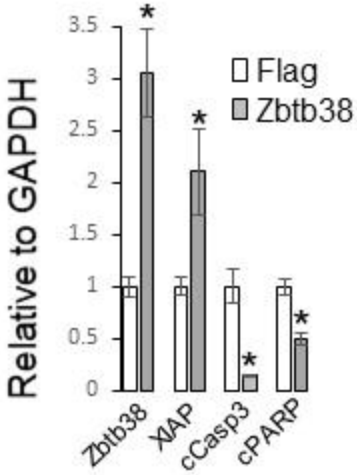

3D C2C12

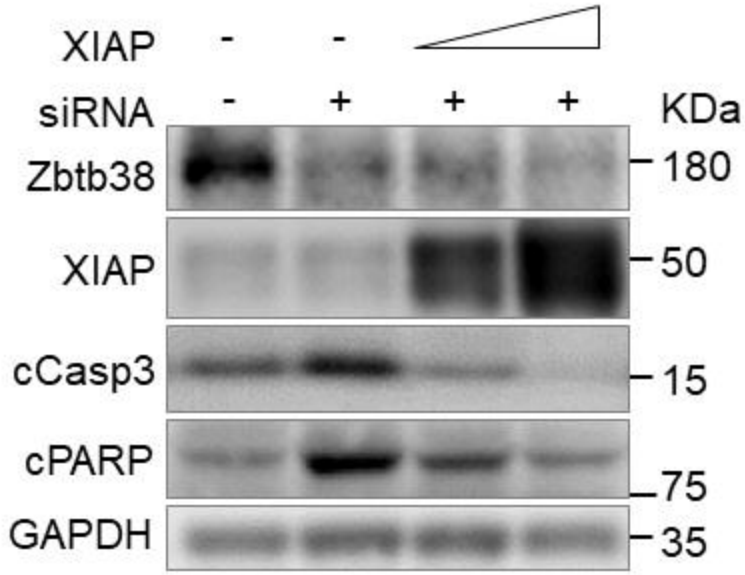

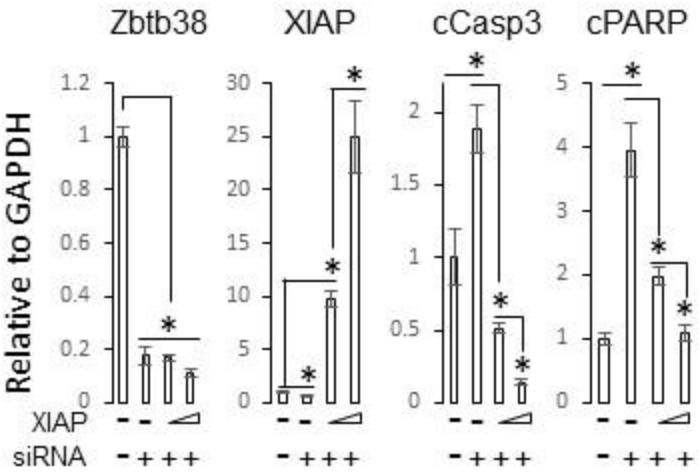

3E *p53 KO*

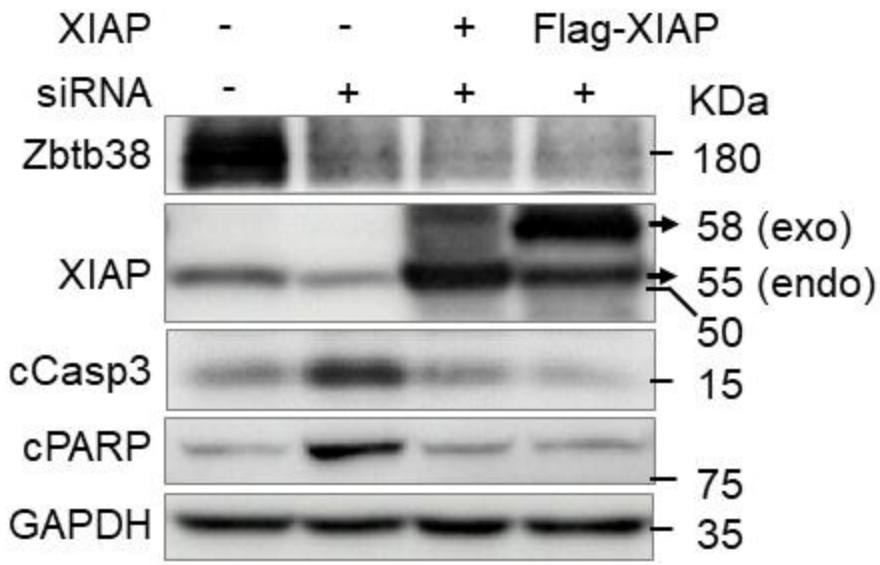

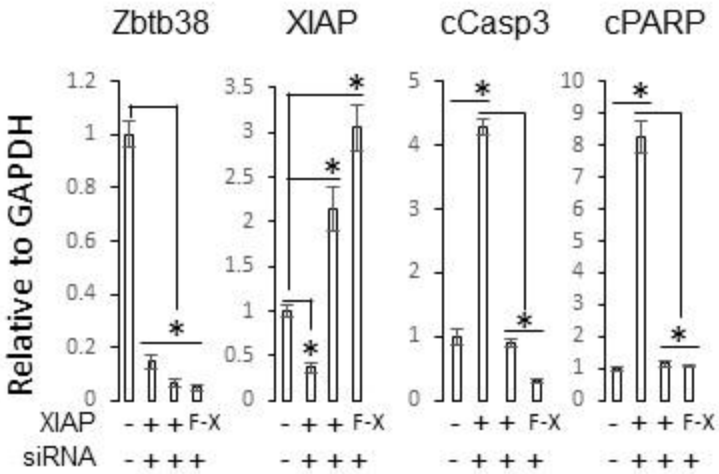

4A

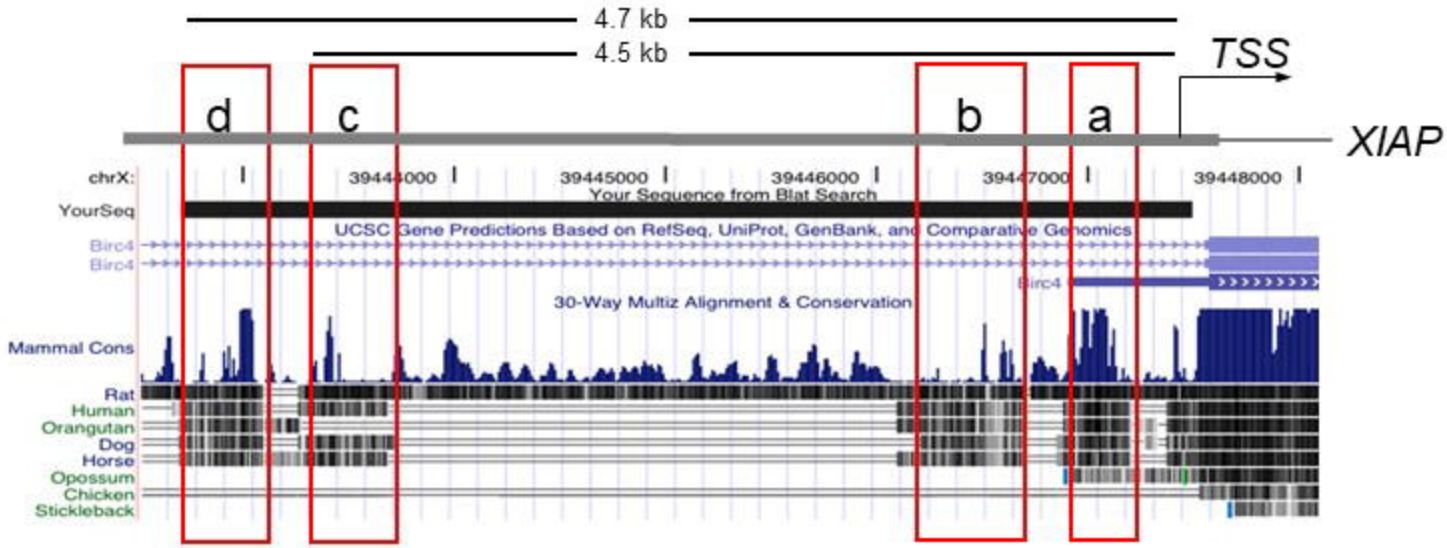
4.7 kb
4.5 kb
TSS
d
c
b
a
XIAP
chrX:
39444000
39445000
39446000
39447000
39448000
YourSeq
Your Sequence from Blat Search
UCSC Gene Predictions Based on RefSeq, UniProt, GenBank, and Comparative Genomics
Birc4
Birc4
Birc4
30-Way Multiz Alignment & Conservation
Mammal Cons
Rat
Human
Orangutan
Dog
Horse
Opossum
Chicken
Stickleback

4B

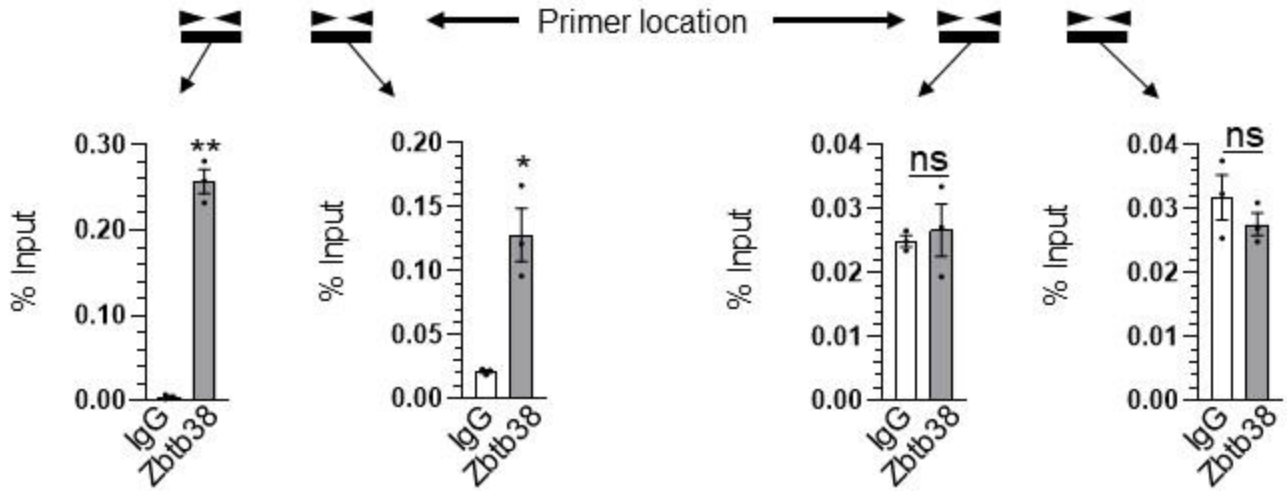
Primer location
% Input
0.30
0.20
0.10
0.00
**
IgG
Zbtb38
0.20
0.15
0.10
0.05
0.00
*
0.04
0.03
0.02
0.01
0.00
ns

4C

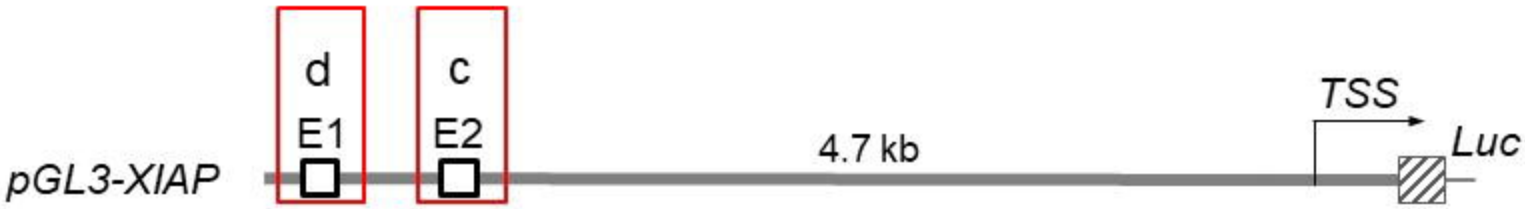

	E-box1	E-box2
Mouse	CACATG	CATCTG
Rat	CACATG	TATCTG
Human	CACATG	CATATA
Dog	CACATG	CATCTG
House	CACATG	CATCTG
wt	CACATG	CATCTG
m1	GTGATG	CATCTG
m1m2	GTGATG	GTGCTG

4D

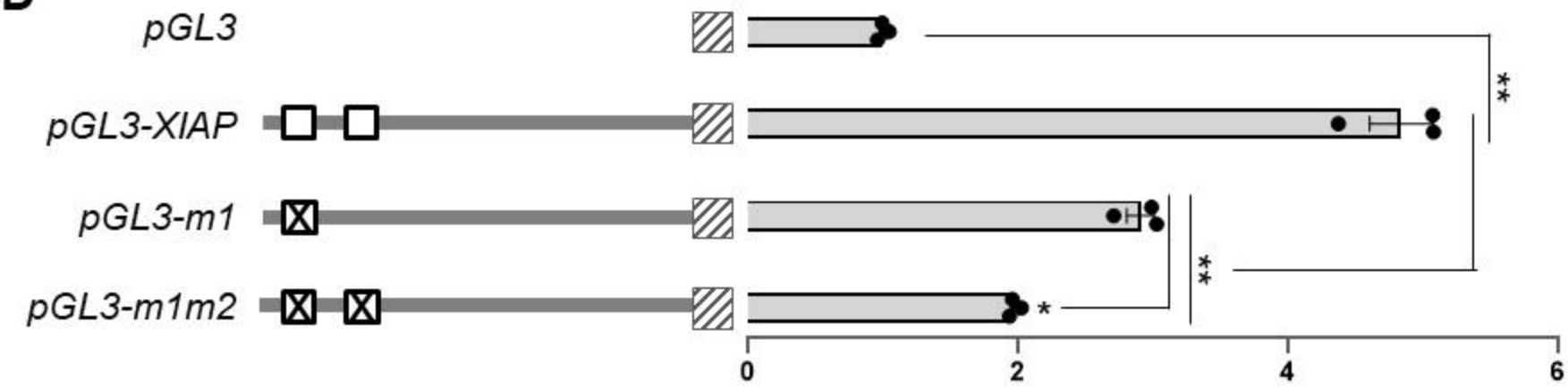

4E

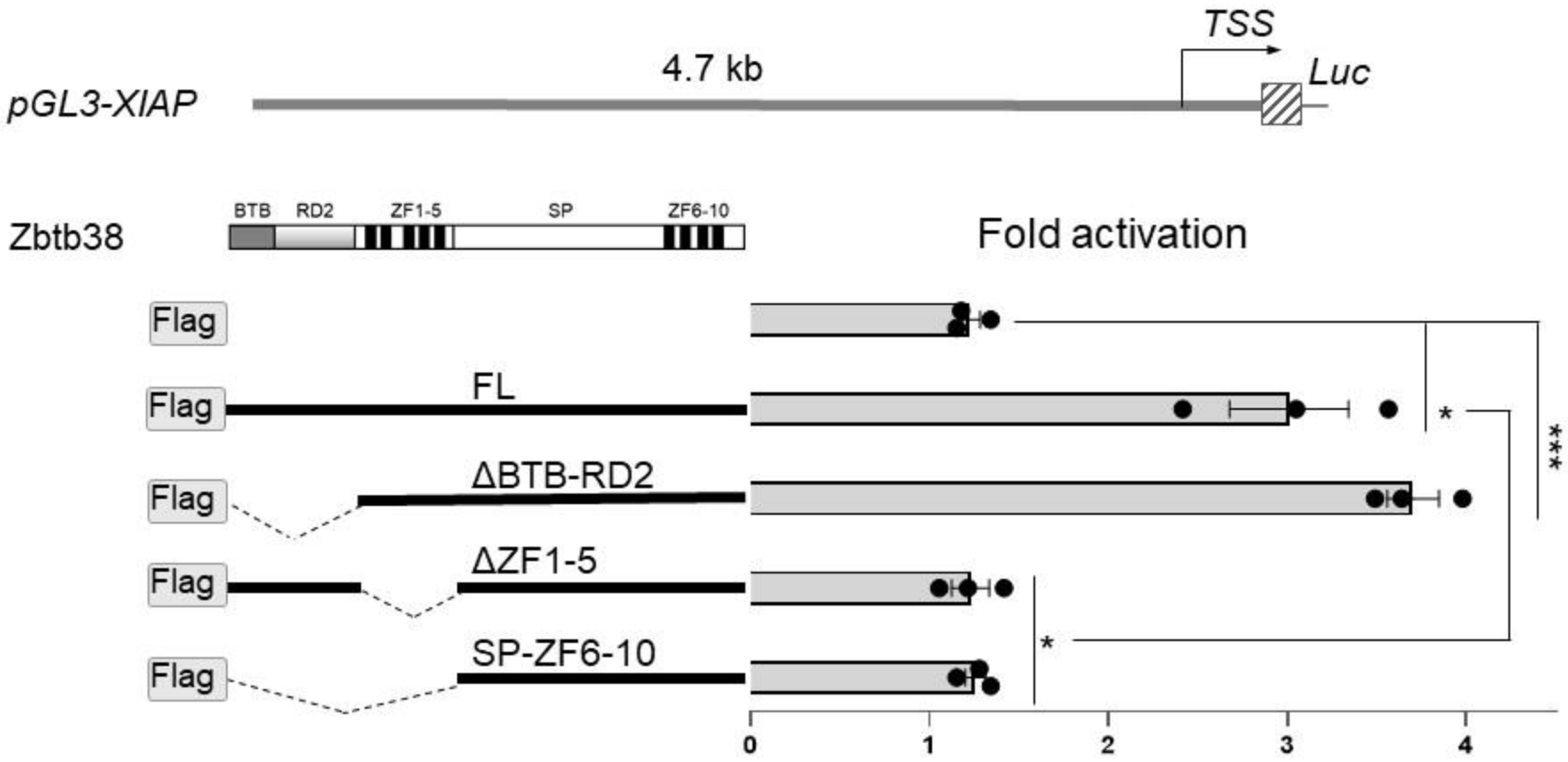
TSS
4.7 kb
Luc
pGL3-XIAP
Zbtb38
BTB
RD2
ZF1-5
SP
ZF6-10
Fold activation
Flag
FL
ΔBTB-RD2
ΔZF1-5
SP-ZF6-10
*
***
0
1
2
3
4

5A

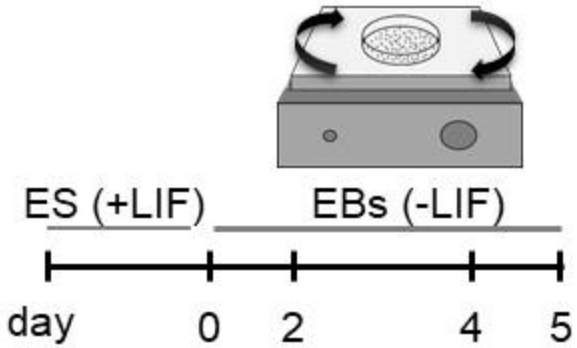
ES (+LIF)
EBs (-LIF)
day
0
2
4
5

5B

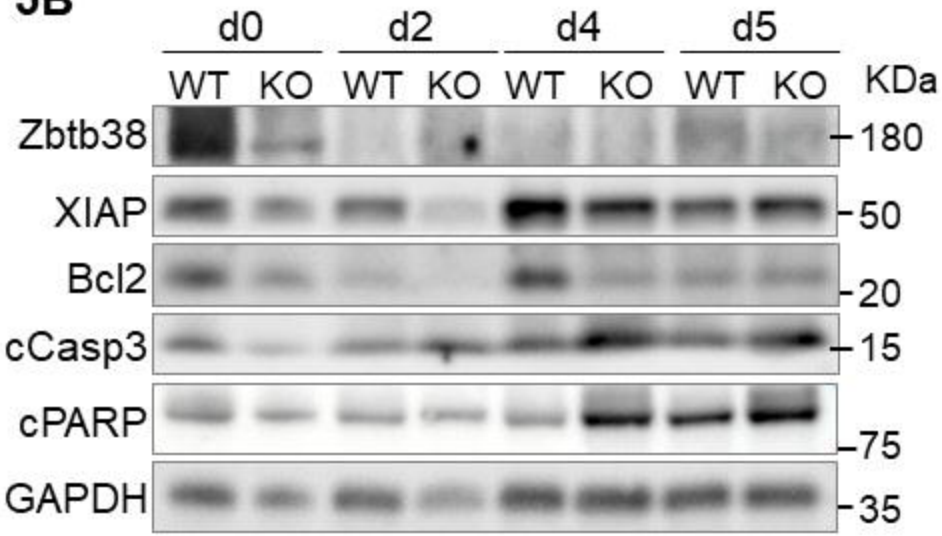
d0
d2
d4
d5
WT
KO
WT
KO
WT
KO
WT
KO
KDa
Zbtb38
XIAP
Bcl2
cCasp3
cPARP
GAPDH
180
50
20
15
75
35

5C

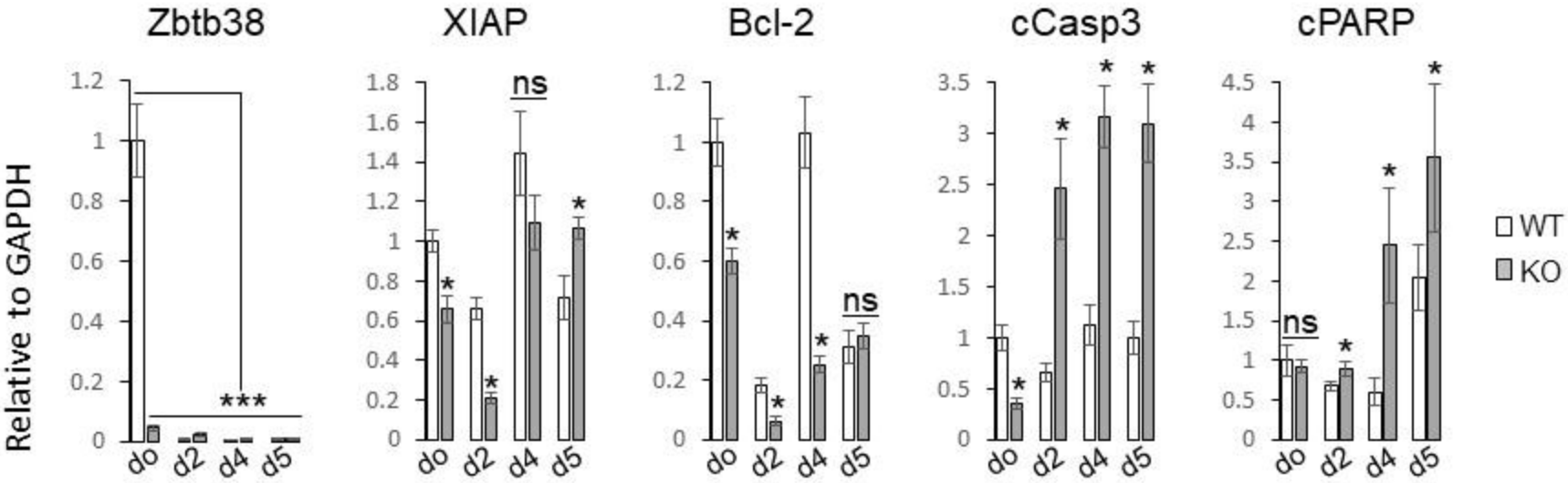
Zbtb38
XIAP
Bcl-2
cCasp3
cPARP
Relative to GAPDH
do
d2
d4
d5
***
ns
*
WT
KO

5D

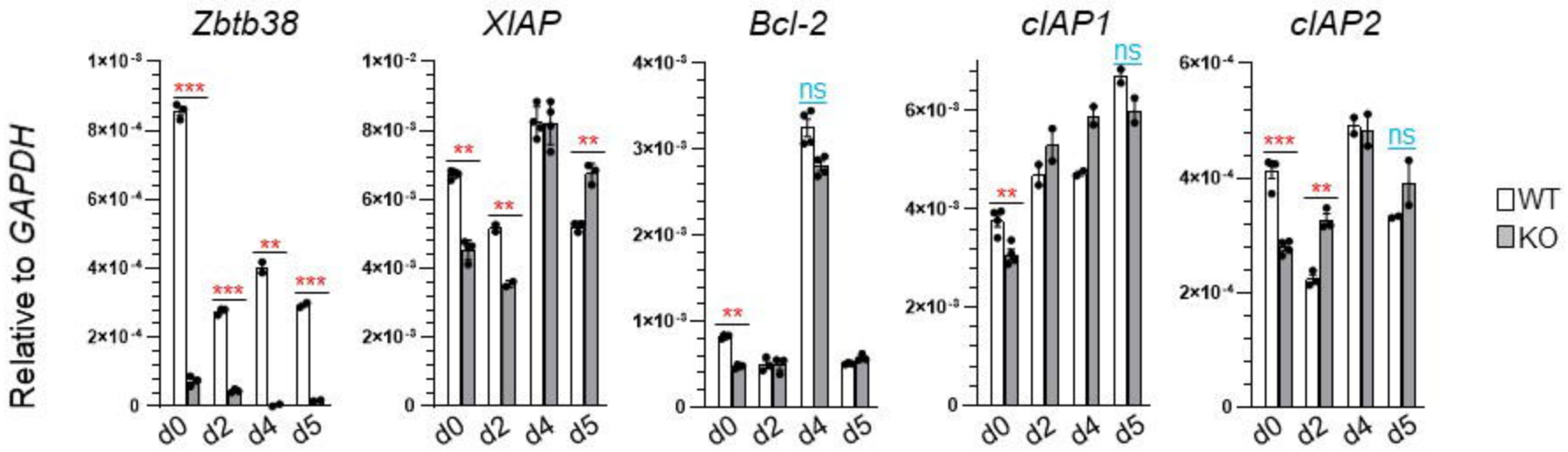
Zbtb38
XIAP
Bcl-2
cIAP1
cIAP2
Relative to GAPDH
1×10⁻³
8×10⁻⁴
6×10⁻⁴
4×10⁻⁴
2×10⁻⁴
0
1×10⁻²
8×10⁻³
6×10⁻³
4×10⁻³
2×10⁻³
4×10⁻³
3×10⁻³
2×10⁻³
1×10⁻³
6×10⁻³
4×10⁻³
2×10⁻³
6×10⁻⁴
4×10⁻⁴
2×10⁻⁴
***
**
ns
d0
d2
d4
d5
WT
KO

5E

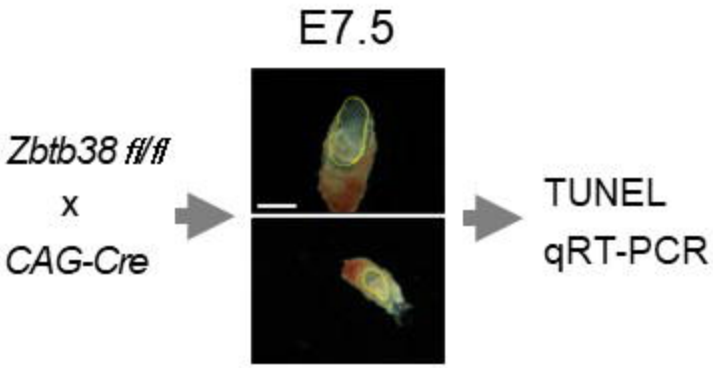
E7.5
Zbtb38 fl/fl
x
CAG-Cre
TUNEL
qRT-PCR

5F

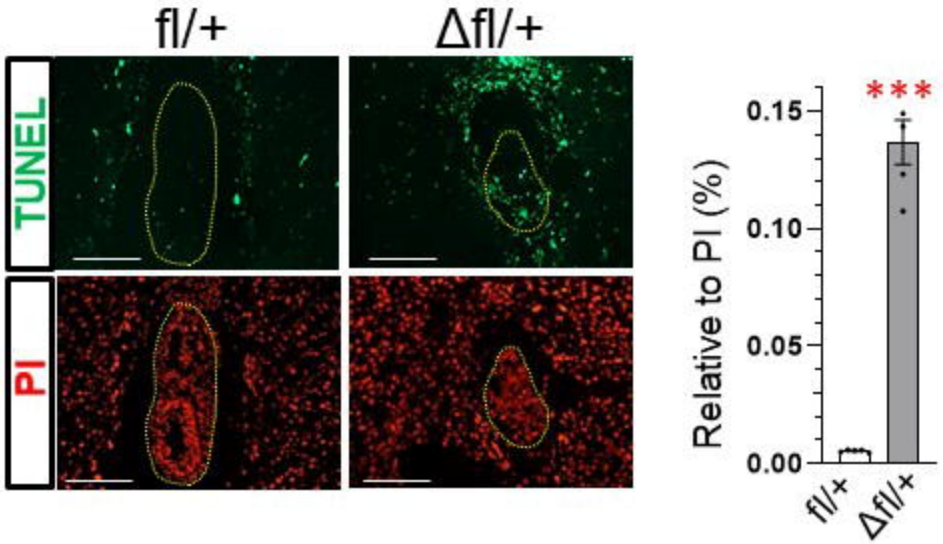
fl/+
Δfl/+
TUNEL
PI
Relative to PI (%)
0.15
0.10
0.05
0.00
***
fl/+
Δfl/+

5G

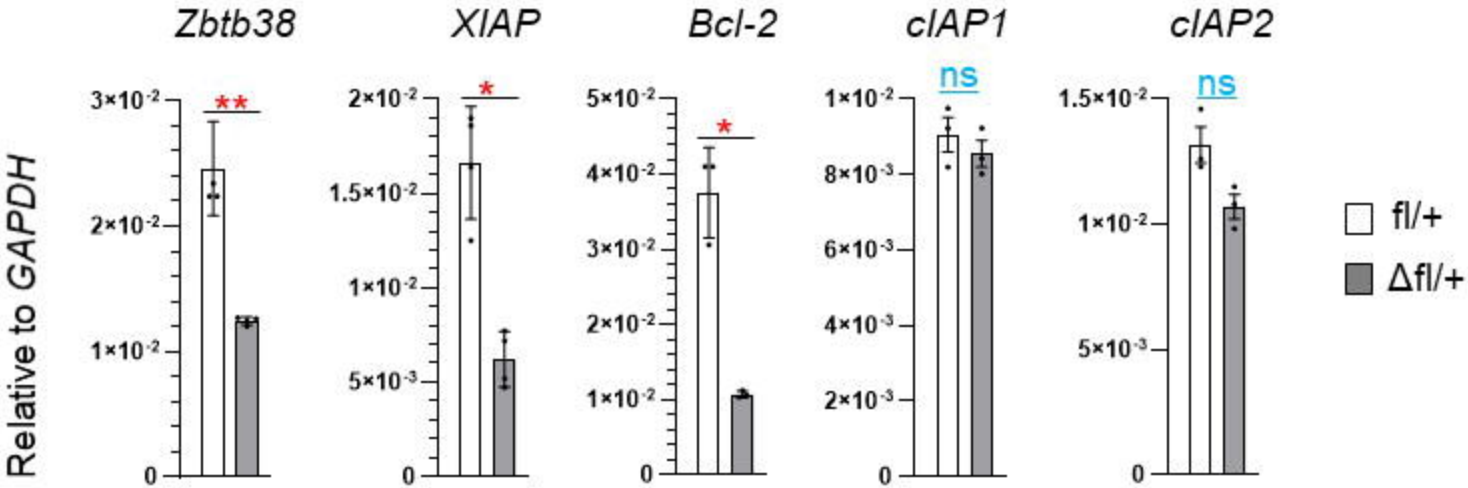
Zbtb38
XIAP
Bcl-2
cIAP1
cIAP2
Relative to GAPDH
3×10-2
2×10-2
1×10-2
0
**
2×10-2
1.5×10-2
1×10-2
5×10-3
0
*
5×10-2
4×10-2
3×10-2
2×10-2
1×10-2
0
*
1×10-2
8×10-3
6×10-3
4×10-3
2×10-3
0
ns
1.5×10-2
1×10-2
5×10-3
0
ns
fl/+
Δfl/+

6

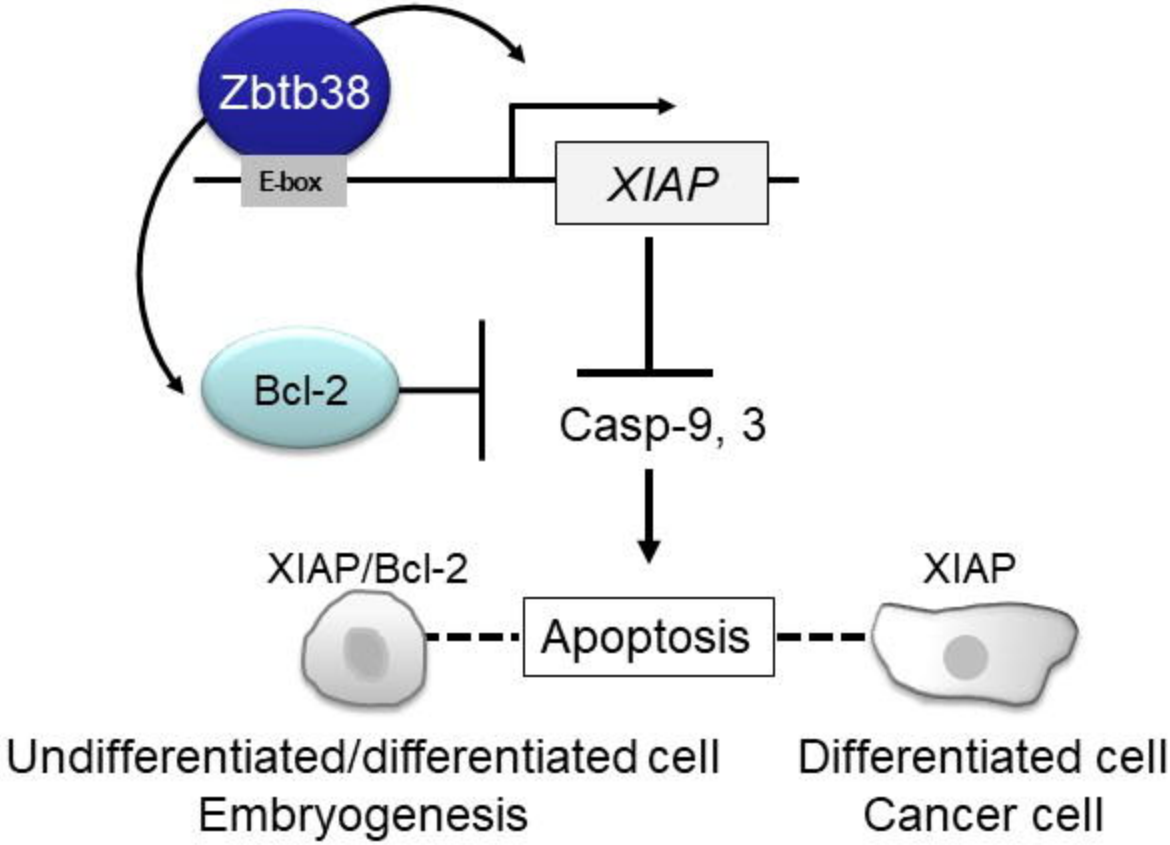
Zbtb38
E-box
XIAP
Bcl-2
Casp-9, 3
XIAP/Bcl-2
Apoptosis
XIAP
Undifferentiated/differentiated cell
Embryogenesis
Differentiated cell
Cancer cell